# Lining-up control strategies for N-trailer vehicles[*]

## Maciej Michałek[†]

Chair of Control and Systems Engineering, Poznan University of Technology (PUT), Piotrowo 3A, 60-965 Poznań, Poland

**Abstract:** Maneuvers performed with tractor-trailers vehicles (N-trailers) belong to the most demanding motion control tasks in the transportation practice. Very frequent maneuvers concern the lining-up process of a vehicle chain, usually as a preliminary stage which prepares the system to subsequent parking/docking maneuvers. The most common lining-up control approach results from utilization of the open-loop asymptotic stability of N-trailer joint-angle dynamics in the forward motion. However, in case of long trailers this approach appears very inefficient especially if the available motion space is substantially limited. By using the triangular forms of joint-angle dynamics the problem of lining-up control for N-trailers is analyzed in the paper by considering two alternative strategies: active lining-up (feedback control) and passive lining-up (open-loop control). The two strategies are compared in the context of their practical effectiveness, and how the effectiveness depends on kinematic parameters of the trailers and their interconnections. It is revealed why the active strategy can be much more efficient in most practical cases. Theoretical considerations are validated by results of numerical simulations and experiments conducted with a laboratory-scale three-trailer robotic vehicle.

**Keywords:** N-trailer vehicles, off-axle hitching, on-axle hitching, feedback control, open-loop control, triangular forms

## 1 Introduction

N-trailers are the most popular articulated vehicles of the ground transportation. They consist of an active tractor equipped with passive trailers [22] connected in series through one of possible hitching types: on-axle or off-axle. N-trailers possess highly nonlinear kinematics with several specific properties (like nonholonomy and under-actuation, structural in-joint-instability during backward motion, and non-minimum-phase property of joint-angle dynamics [17]) which make them especially unintuitive and difficult systems to manual control. N-trailer vehicles can be divided into three categories: standard N-trailers (SNT, see [9], [10]) where all the trailers are hitched exactly at a mid-point of a preceding wheels axle (on-axle hitching), non-standard N-trailers (nSNT, cf. [16]) where all the trailers are hitched off the preceding wheels axle (off-axle hitching), and general N-trailers (GNT, see [1]) characterized by combined on-axle and off-axle types of hitching for particular trailers. In the literature one can

find papers which treat the classical motion control problems for different types of N-trailer vehicles (see e.g. [2], [11], [12], [24], [4], [16], [6], [22]). Especially numerous studies can be found for vehicles with strictly limited number of trailers – see e.g. [25], [21], [7], [28], [13], [5], [3].

In practice, one of the most frequent maneuvers with N-trailers result from the lining-up process of a vehicle chain. Proper alignment of the vehicle segments is often a prerequisite to successfully perform such difficult maneuvers like backward docking with trailers. Due to practical limitations of an available obstacle-free space, the lining-up process should be usually completed along a reasonably short distance which a *distinguished vehicle segment*[1] has to pass. The common approach to the vehicle lining-up control is to utilize the open-loop asymptotic-stability property of the joint-angle dynamics, where the tractor is driven forward with zero angular velocity until a vehicle lines-up with a prescribed precision. It is in fact a passive (open-loop) control strategy, where a tractor segment does not change a sign of a longitudinal velocity during the whole control process. This simple approach can be however unacceptable for vehicles with long trailers, because the lining-up process may involve in this case excessively long distance of the tractor motion. It turns out that one can propose an alternative lining-up strategy which can be more efficient in comparison to the passive one. In this paper the active lining-up strategy is proposed for N-trailers by using a closed-loop control with feedback from particular joint angles. Simple conditions are formulated under which the active strategy becomes more efficient – it requires much less distance to be passed by a distinguished segment. Formal analysis and comparison of the two lining-up strategies are presented by using the lower- and upper-triangular forms [8, 26, 27] of joint-angle dynamics. Triangular forms allows one to reveal how a rate of convergence for particular control strategies depend on parameters of trailers and their interconnections. The main theoretical results are devised for nSNT vehicles. It is shown however, that after simple modifications both control strategies can be practically applied also into GNT and SNT vehicles.

This work is a substantial extension of the conference paper [15]. The new results comprise a quantitative studies and comparison of the lining-up strategies, additional details of the formal stability analysis, applicability of the

---

[†]Corresponding author e-mail: `maciej.michalek@put.poznan.pl`

[1]By the *distinguished vehicle segment* one understands either a tractor or a last trailer according to a type of the lining-up strategy considered (see Section 4).

active lining-up method into GNT and SNT kinematics, as well as experimental validation of the active lining-up strategy. The paper is organized as follows. After description of the N-trailer kinematics and formulation of the control problem in Section 2, the triangular forms of the kinematics are presented in Section 3. Lining-up strategies are proposed in Section 4 followed by a formal stability analysis, by quantitative studies, and by applicability extensions in Section 5. Numerical and experimental validation is a topic of Section 6. The paper is concluded in Section 7.

## 2 N-trailer kinematics and problem formulation

### 2.1 Derivation of N-trailer kinematics

Kinematics of the N-trailer vehicle can be derived upon the interconnected-body chain presented in Fig. 1, where the vehicle configuration variables have been defined. The N-trailer consists of a differentially-driven tractor (the only active segment numbered by zero) and a number of $N$ trailers (numbered from 1 to $N$) interconnected by passive rotary joints. The length of an $i$-th trailer, $i = 1, \ldots, N$, is denoted by parameter $L_i > 0$. Every $i$-th joint is located on a preceding segment in some distance from a wheels axle called the *hitching offset* $L_{hi}$. In general, hitching offsets can be either non-zero (*off-axle* hitching) or equal to zero (*on-axle* hitching). Let us assume a positive value of parameter $L_{hi}$ if the $i$-th joint is located *behind* a preceding wheels axle; consequently, $L_{hi}$ is treated as negative if the $i$-th joint is situated *in front* of the preceding wheels axle. One defines two control inputs of the vehicle: $\omega_0$ (angular tractor velocity), and $v_0$ (longitudinal velocity of the mid-point of a tractor wheels axle). A kinematic model of the N-trailer will be derived in the sequel for a general case without any assumption on the hitching type of trailers (off- or on-axle).

Configuration of the N-trailer can be uniquely determined by the following $N + 3$ independent variables:

$$\boldsymbol{q} \triangleq [\beta_1 \ \ldots \ \beta_N \ \theta_N \ x_N \ y_N]^\top = \begin{bmatrix} \boldsymbol{\beta} \\ \boldsymbol{q}_N \end{bmatrix}, \qquad (1)$$

where $\boldsymbol{\beta} = [\beta_1 \ \ldots \ \beta_N] \in \mathbb{R}^N$ is a vector of joint angles, and $\boldsymbol{q}_N = [\theta_N \ x_N \ y_N]^\top \in \mathbb{R}^3$ is a posture of the last vehicle segment (orientation angle and position coordinates of point $P$, respectively, depicted in Fig. 1).

According to Fig. 1, and under assumption of the rolling-without-skidding motion for each of the vehicle wheels, one may treat every $i$-th vehicle segment ($i = 0, 1, \ldots, N$) as the unicycle[2]

$$\dot{\theta}_i = \omega_i, \quad \dot{x}_i = v_i c\theta_i, \quad \dot{y}_i = v_i s\theta_i \qquad (2)$$

with virtual inputs $\omega_i$ and $v_i$ being the angular and longitudinal velocities of the $i$-th segment, respectively. Note

---

[2]From now on the more compact notation will be used: $s\alpha \equiv \sin \alpha$, $c\alpha \equiv \cos \alpha$.
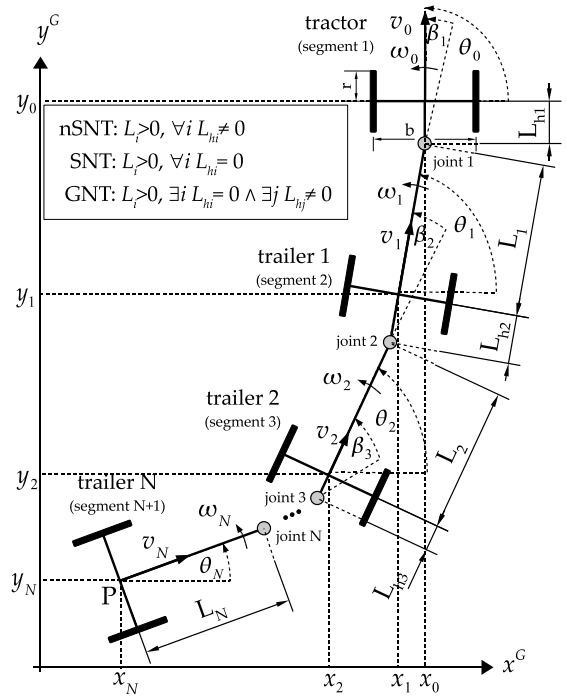


Figure 1: Kinematic chain of the N-trailer with definition of configuration variables, control inputs, and vehicle parameters (positive hitching offsets $L_{hi}$ are denoted)

that by taking $i = 0$ in (2) one obtains the tractor kinematics with only physically available control inputs $\omega_0, v_0$. Defining the velocity vector

$$\boldsymbol{u}_i \triangleq [\omega_i \ v_i]^\top \in \mathbb{R}^2 \qquad (3)$$

one can formulate a simple formula relating velocities of any two consecutive interconnected segments in a vehicle chain

$$\boldsymbol{u}_i = \boldsymbol{J}_i(\beta_i)\boldsymbol{u}_{i-1}, \quad i = 1, \ldots, N, \qquad (4)$$

where

$$\boldsymbol{J}_i(\beta_i) = \begin{bmatrix} -\frac{L_{hi}}{L_i}c\beta_i & \frac{1}{L_i}s\beta_i \\ L_{hi}s\beta_i & c\beta_i \end{bmatrix} \qquad (5)$$

is the velocity transformation matrix. Using equation (4) one obtains the following velocity propagation formula relating velocity vector $\boldsymbol{u}_i$ of any $i$-th segment ($i = 1, \ldots, N$) with tractor control input $\boldsymbol{u}_0 = [\omega_0 \ v_0]^\top$:

$$\boldsymbol{u}_i = \prod_{j=i}^{1} \boldsymbol{J}_j(\beta_j)\boldsymbol{u}_0 \qquad (6)$$

$$= \boldsymbol{J}_i(\beta_i)\boldsymbol{J}_{i-1}(\beta_{i-1}) \ldots \boldsymbol{J}_1(\beta_1)\boldsymbol{u}_0.$$

Additional kinematic relation results from definition of the $i$-th joint angle $\beta_i \triangleq \theta_{i-1} - \theta_i$ (cf. Fig. 1) which, after its time-differentiation and utilization of Eq. (2), yields

$$\dot{\beta}_i = \omega_{i-1} - \omega_i. \qquad (7)$$

Now, by using definition (3) and combining (2), (6), and (7) one can formulate kinematics of the N-trailer vehicle in a closed form as a driftless system with control input $\boldsymbol{u}_0 = [\omega_0 \ v_0]^\top$

$$\dot{\boldsymbol{q}} = \begin{bmatrix} \dot{\boldsymbol{\beta}} \\ \dot{\boldsymbol{q}}_N \end{bmatrix} = \begin{bmatrix} \boldsymbol{S}_\beta(\boldsymbol{\beta}) \\ \boldsymbol{S}_N(\boldsymbol{\beta}, \boldsymbol{q}_N) \end{bmatrix} \boldsymbol{u}_0 = \boldsymbol{S}(\boldsymbol{q})\boldsymbol{u}_0. \qquad (8)$$

System (8) can be decomposed, respectively, into the joint-angle subsystem ($\beta$-subsystem) and the posture subsystem ($q_N$-subsystem)

$$\dot{\boldsymbol{\beta}} = \boldsymbol{S}_\beta(\boldsymbol{\beta})\boldsymbol{u}_0, \tag{9}$$

$$\dot{\boldsymbol{q}}_N = \boldsymbol{S}_N(\boldsymbol{\beta}, \boldsymbol{q}_N)\boldsymbol{u}_0, \tag{10}$$

where

$$\boldsymbol{S}_\beta(\boldsymbol{\beta}) = \begin{bmatrix} \boldsymbol{a}^\top (\boldsymbol{I} - \boldsymbol{J}_1(\beta_1)) \\ \vdots \\ \boldsymbol{a}^\top (\boldsymbol{I} - \boldsymbol{J}_i(\beta_i)) \prod_{j=i-1}^{1} \boldsymbol{J}_j(\beta_j) \\ \vdots \\ \boldsymbol{a}^\top (\boldsymbol{I} - \boldsymbol{J}_N(\beta_N)) \prod_{j=N-1}^{1} \boldsymbol{J}_j(\beta_j) \end{bmatrix}, \tag{11}$$

with $\boldsymbol{I} \in \mathbb{R}^{2\times 2}$ being a unit matrix, and

$$\boldsymbol{S}_N(\boldsymbol{\beta}, \boldsymbol{q}_N) = \begin{bmatrix} \boldsymbol{a}^\top \prod_{j=N}^{1} \boldsymbol{J}_j(\beta_j) \\ \boldsymbol{d}^\top \prod_{j=N}^{1} \boldsymbol{J}_j(\beta_j) \mathrm{c}\theta_N \\ \boldsymbol{d}^\top \prod_{j=N}^{1} \boldsymbol{J}_j(\beta_j) \mathrm{s}\theta_N \end{bmatrix} \tag{12}$$

with $\boldsymbol{a}^\top \triangleq [1\ 0]$ and $\boldsymbol{d}^\top \triangleq [0\ 1]$. Kinematic model represented by (8) remains valid regardless what types of hitching have been used in a vehicle (it admits $L_{hi} = 0$ as well as $L_{hi} \neq 0$). Thus, equation (8) describes kinematics of all the N-trailers (SNT, nSNT, and GNT) in a unified manner.

In the special case of nSNT vehicles, where all the hitching offsets $L_{hi}$ are non-zero, it is possible to find the inverse relation to (4) in the form

$$\boldsymbol{u}_{i-1} = \boldsymbol{J}_i^{-1}(\beta_i)\boldsymbol{u}_i, \quad i = 1, \ldots, N, \tag{13}$$

where the inverse matrix

$$\boldsymbol{J}_i^{-1}(\beta_i) = \begin{bmatrix} -\frac{L_i}{L_{hi}}\mathrm{c}\beta_i & \frac{1}{L_{hi}}\mathrm{s}\beta_i \\ L_i\mathrm{s}\beta_i & \mathrm{c}\beta_i \end{bmatrix} \tag{14}$$

is always well determined if $L_{hi} \neq 0$. By using equation (13) one can simply derive the velocity propagation formula relating velocity vector $\boldsymbol{u}_{i-1}$ of any $(i-1)$-st segment with velocity vector $\boldsymbol{u}_N = [\omega_N\ v_N]^\top$ of the last trailer:

$$\boldsymbol{u}_{i-1} = \prod_{j=i}^{N} \boldsymbol{J}_j^{-1}(\beta_j)\boldsymbol{u}_N \tag{15}$$

$$= \boldsymbol{J}_i^{-1}(\beta_i)\boldsymbol{J}_{i+1}^{-1}(\beta_{i+1})\ldots\boldsymbol{J}_N^{-1}(\beta_N)\boldsymbol{u}_N.$$

Propagation formula (15) will play a key role in the *active* lining-up control strategy proposed in Section 4.1.

## 2.2 Control problem formulation

Before stating the control objective let us formulate two assumptions which will restrict the types of considered N-trailers described by (8):

A1. all the hitching offsets in kinematics (8) are nonzero:
$\forall i\ L_{hi} \neq 0$,

A2. all the nonzero hitching offsets in kinematics (8) have a common sign reflected by $\sigma \in \{-1, +1\}$, where

$$\sigma \triangleq \mathrm{sgn}(L_{hi}) = \mathrm{sgn}(L_{hi-1}), \quad i = 2, \ldots, N. \tag{16}$$

Assumption A1 limits a set of N-trailers to the nSNT class, for which the inverse matrix (14) and propagation formula (15) are well determined and bounded. Assumption A2 defines the *homogeneous hitching* requirement, which concerns only the signs of the hitching offsets – it does not preclude different absolute values of particular offsets. Assumption A2 is crucial for the active lining-up strategy considered in the paper – except for a some special case (see Section 5.2) it cannot be repealed. On the other hand, it will be shown in Section 5 that assumption A1 is much less stringent allowing one to apply the lining-up methods also into the GNT and SNT vehicles.

The control objective considered in the paper can be formulated as follows.

**Problem 1 (Control objective)** *For the $\beta$-subsystem (9) of N-trailer kinematics (8) satisfying assumptions A1-A2 find a bounded control function $\boldsymbol{u}_0(\cdot)$ which, after its application into (8), guarantees that for all initial conditions $\|\boldsymbol{\beta}(0)\|$ sufficiently close to zero the joint-angle dynamics (9) is locally stable and*

$$\forall t \geq T\ \ \|\boldsymbol{\beta}(t)\| \leq \epsilon, \tag{17}$$

*where $\epsilon \geq 0$ is a prescribed constant, and $T \in [0, \infty)$ is the lining-up time-horizon.*

The above control task admits two kinds of local stability: *practical stability* for $\epsilon > 0$, $T < \infty$, and *asymptotic stability* for $\epsilon = 0$ and $T \leq \infty$.

Since one considers the vehicle lining-up problem, the $\beta$-subsystem represented by (9) is of a particular interest. Time-evolution of the posture subsystem (10) has a secondary meaning. However from a practical standpoint one should expect acceptable behavior also for $q_N$-subsystem being a part of a whole vehicle configuration. This issue will be commented on in Section 4.

## 3 Triangular forms of joint-angle sybsystem

In order to solve Problem 1 let us first express the joint-angle subsystem (9) in the lower- and upper-triangular normal forms.

### 3.1 Lower-triangular form with input $\boldsymbol{u}_0$

Recalling the terms used in model (9) with matrix (11), let us introduce the auxiliary matrix

$$\boldsymbol{F}_i(\beta_i) \triangleq \boldsymbol{I} - \boldsymbol{J}_i(\beta_i) = \begin{bmatrix} 1 + \frac{L_{hi}}{L_i}\mathrm{c}\beta_i & -\frac{1}{L_i}\mathrm{s}\beta_i \\ -L_{hi}\mathrm{s}\beta_i & 1 - \mathrm{c}\beta_i \end{bmatrix} \tag{18}$$

with $\boldsymbol{J}_i(\beta_i)$ defined by (5). It can be easily found that subsystem (9) can be expressed in the special normal form

with input $\boldsymbol{u}_0$ as follows:

$$\dot{\beta}_1 = \boldsymbol{f}_1^\top(\beta_1)\boldsymbol{u}_0$$
$$\dot{\beta}_2 = \boldsymbol{f}_2^\top(\beta_1, \beta_2)\boldsymbol{u}_0$$
$$\vdots \qquad\qquad (19)$$
$$\dot{\beta}_{N-1} = \boldsymbol{f}_{N-1}^\top(\beta_1, \beta_2, \beta_3, \ldots, \beta_{N-1})\boldsymbol{u}_0$$
$$\dot{\beta}_N = \boldsymbol{f}_N^\top(\beta_1, \beta_2, \beta_3, \ldots, \beta_{N-1}, \beta_N)\boldsymbol{u}_0,$$

where

$$\boldsymbol{f}_1^\top(\beta_1) = \boldsymbol{a}^\top \boldsymbol{F}_1(\beta_1) = \begin{bmatrix} 1 + \frac{L_{h1}\mathrm{c}\beta_1}{L_1} & \frac{-\mathrm{s}\beta_1}{L_1} \end{bmatrix}, \qquad (20)$$

and for $i = 2, \ldots, N$

$$\boldsymbol{f}_i^\top(\beta_1, \ldots, \beta_i) = \boldsymbol{a}^\top \boldsymbol{F}_i(\beta_i) \prod_{j=i-1}^{1} \boldsymbol{J}_j(\beta_j) \qquad (21)$$
$$= \begin{bmatrix} 1 + \frac{L_{hi}\mathrm{c}\beta_i}{L_i} & \frac{-\mathrm{s}\beta_i}{L_i} \end{bmatrix} \boldsymbol{J}_F(\beta_1, \ldots, \beta_{i-1})$$

with $\boldsymbol{J}_F(\beta_1, \ldots, \beta_{i-1}) \triangleq \prod_{j=i-1}^{1} \boldsymbol{J}_j(\beta_j)$. The set of equations (19) represents the joint-angle dynamics in the lower-triangular form[3] [8,26], where the $i$-th equation depends on the $i$-th joint angle and on all the preceding ones with indexes $1, \ldots, i-1$, while it does not depend on any variables with indexes greater than $i$. In this way one can treat all the terms related to the variables with smaller indexes appearing on the right-hand side of the $i$-th equation as *external disturbances* to the *nominal* dynamics $\dot{\beta}_i = \tilde{\boldsymbol{f}}_i^\top(\beta_i)\boldsymbol{u}_0$ dependent only on $\beta_i$ and input $\boldsymbol{u}_0$. Note that the above lower-triangular form includes control input $\boldsymbol{u}_0$ which is directly available in the tractor.

### 3.2 Upper-triangular form with input $\boldsymbol{u}_N$

In order to obtain an upper-triangular form one has to redefine the control input by replacing $\boldsymbol{u}_0$ used in (9) with velocity vector $\boldsymbol{u}_N = [\omega_N \ v_N]^\top$ treated as a virtual control input. It is worth to emphasize that although $\boldsymbol{u}_N$ cannot be directly manipulated, thus at the first look the above proposition could seem impractical, it can be indirectly (but precisely and instantaneously[4]) forced with tractor input $\boldsymbol{u}_0$ by using relation (15) for $i = 1$:

$$\boldsymbol{u}_0(\boldsymbol{\beta}) = \prod_{j=1}^{N} \boldsymbol{J}_j^{-1}(\beta_j)\boldsymbol{u}_N. \qquad (22)$$

Satisfaction of assumption A1 guarantees invertability of matrices $\boldsymbol{J}_j(\beta_j)$ making (22) well determined for all $\boldsymbol{\beta} \in \mathbb{R}^N$. Since (22) is an algebraic transformation, one may treat $\boldsymbol{u}_N$ as an alternative input to the joint-angle subsystem. Introducing the auxiliary matrix

$$\boldsymbol{B}_i(\beta_i) \triangleq \boldsymbol{J}_i^{-1}(\beta_i) - \boldsymbol{I} = \begin{bmatrix} -1 - \frac{L_i}{L_{hi}}\mathrm{c}\beta_i & \frac{1}{L_{hi}}\mathrm{s}\beta_i \\ L_i\mathrm{s}\beta_i & \mathrm{c}\beta_i - 1 \end{bmatrix} \quad (23)$$

---

[3]Since equations (19) directly result from the general form of N-trailer kinematics (8), they remain valid for all the types of N-trailers (nSNT, GNT and SNT).

[4]Instantaneous forcing of input $\boldsymbol{u}_0$ relates to the case where one considers control solely on the kinematic level. In practice, where the higher-order dynamics of a vehicle reveal, the inevitable actuator transients appear and must be accepted (see e.g. [20]).

one may rewrite $\beta$-subsystem (9) in the upper-triangular form[5] with input $\boldsymbol{u}_N$ as follows:

$$\dot{\beta}_1 = \boldsymbol{b}_1^\top(\beta_1, \beta_2, \beta_3, \ldots, \beta_{N-1}, \beta_N)\boldsymbol{u}_N$$
$$\dot{\beta}_2 = \boldsymbol{b}_2^\top(\beta_2, \beta_3, \ldots, \beta_{N-1}, \beta_N)\boldsymbol{u}_N$$
$$\vdots \qquad\qquad (24)$$
$$\dot{\beta}_{N-1} = \boldsymbol{b}_{N-1}^\top(\beta_{N-1}, \beta_N)\boldsymbol{u}_N$$
$$\dot{\beta}_N = \boldsymbol{b}_N^\top(\beta_N)\boldsymbol{u}_N,$$

where

$$\boldsymbol{b}_N^\top(\beta_N) = \boldsymbol{a}^\top \boldsymbol{B}_N(\beta_N) = \begin{bmatrix} -1 - \frac{L_N\mathrm{c}\beta_N}{L_{hN}} & \frac{\mathrm{s}\beta_N}{L_{hN}} \end{bmatrix}, \quad (25)$$

and for $i = 1, \ldots, N-1$

$$\boldsymbol{b}_i^\top(\beta_i, \ldots, \beta_N) = \boldsymbol{a}^\top \boldsymbol{B}_i(\beta_i) \prod_{j=i+1}^{N} \boldsymbol{J}_j^{-1}(\beta_j) \qquad (26)$$
$$= \begin{bmatrix} -1 - \frac{L_i\mathrm{c}\beta_i}{L_{hi}} & \frac{\mathrm{s}\beta_i}{L_{hi}} \end{bmatrix} \boldsymbol{J}_B(\beta_{i+1}, \ldots, \beta_N)$$

with $\boldsymbol{J}_B(\beta_{i+1}, \ldots, \beta_N) \triangleq \prod_{j=i+1}^{N} \boldsymbol{J}_j^{-1}(\beta_j)$. In this case the $i$-th equation depends on the $i$-th joint angle and on all the following ones with indexes $i+1, \ldots, N$, while it does not depend on any variables with indexes smaller than $i$. By analogy to the case presented in Section 3.1 one can treat all the terms with indexes greater than $i$ appearing on the right-hand side of the $i$-th equation as *external disturbances* to the *nominal* dynamics $\dot{\beta}_i = \tilde{\boldsymbol{b}}_i^\top(\beta_i)\boldsymbol{u}_N$ dependent only on $\beta_i$ and input $\boldsymbol{u}_N$.

## 4 Active and passive lining-up strategies

In this section, two alternative lining-up control strategies called *active lining-up* and *passive lining-up* will be considered. A main differentiation between active and passive strategies depends on the way the vehicle control input $\boldsymbol{u}_0$ is designed. The active strategy will be designed using the upper-triangular form (24) by appropriate definition of the virtual control input $\boldsymbol{u}_N$ and then by application of the *feedback control* function $\boldsymbol{u}_0 := \boldsymbol{u}_0(\boldsymbol{\beta})$ according to transformation (22). The passive strategy – widely known from practical experience – will be determined using an *open-loop control* policy by direct definition of the tractor input $\boldsymbol{u}_0$. In the latter case, the lining-up effect will be a consequence of asymptotic stability of the lower-triangular joint-angle dynamics (19) in the forward vehicle motion.

### 4.1 Active lining-up strategy

Let us define the active lining-up control strategy by the following proposition.

**Proposition 1 (Active lining-up)** *Assume that N-trailer kinematics satisfy A1-A2. Then the feedback control law*

$$\boldsymbol{u}_0(\boldsymbol{\beta}) = \begin{bmatrix} \omega_0(\boldsymbol{\beta}) \\ v_0(\boldsymbol{\beta}) \end{bmatrix} \triangleq \prod_{j=1}^{N} \boldsymbol{J}_j^{-1}(\beta_j)\boldsymbol{u}_N \qquad (27)$$

---

[5]In the literature called also the *feedforward form* [27].

*with virtual control input*

$$\boldsymbol{u}_N = \begin{bmatrix} \omega_N \\ v_N \end{bmatrix} \triangleq \begin{bmatrix} 0 \\ v_N \end{bmatrix} \qquad (28)$$

*determined by*

$$v_N \triangleq \begin{cases} -\sigma\,\bar{v}_N & for \quad \|\boldsymbol{\beta}\| > \epsilon \\ 0 & for \quad \|\boldsymbol{\beta}\| \le \epsilon \end{cases}, \quad 0 < \bar{v}_N < \infty \quad (29)$$

*applied into kinematics (8) solves Problem 1 and will be called the* active lining-up *strategy.*

**Proof 1** *First, let us show boundedness of control input (27) by the following estimation:*

$$\|\boldsymbol{u}_0(\boldsymbol{\beta})\| \stackrel{(27)}{=} \left\| \prod_{j=1}^{N} \boldsymbol{J}_j^{-1}(\beta_j)\boldsymbol{u}_N \right\|$$

$$\le \prod_{j=1}^{N} \|\boldsymbol{J}_j^{-1}(\beta_j)\| \|\boldsymbol{u}_N\| \stackrel{(29)}{=} \prod_{j=1}^{N} M_j \bar{v}_N < \infty,$$

*where* $M_j = \sqrt{\left(1 + \frac{L_j^2}{L_{hj}^2}\right)\mathrm{c}^2\beta_j + \left(\frac{1}{L_{hj}^2} + L_j^2\right)\mathrm{s}^2\beta_j}$ *is the Frobenius norm[6] of matrix* $\boldsymbol{J}_j^{-1}(\beta_j)$, *which is bounded under assumption A1.*

*Second, let us analyze stability of the closed-loop system. The right-hand side of definition (27) – cf. with (22) – is an algebraic mapping well determined for all* $\beta_i$, $i = 1, \ldots, N$ *under assumption A1. Thus, application of control input (27) into joint-angle kinematics (9) is equivalent to application of virtual control input (28) into kinematics represented by (24). As a consequence, one can limit the stability analysis to the system in the upper-triangular form (24) with input* $\boldsymbol{u}_N$ *defined by (28)-(29).*

*Let us first consider the case with* $\epsilon = 0$ *in (29). Recalling (26) and (25) one can rewrite dynamics (24) in the compact form*

$$\dot{\beta}_i = \begin{bmatrix} -(1 + \frac{L_i \mathrm{c}\beta_i}{L_{hi}}) & \frac{\mathrm{s}\beta_i}{L_{hi}} \end{bmatrix} \boldsymbol{J}_B(\beta_{i+1}, \ldots, \beta_N)\boldsymbol{u}_N, \quad (30)$$

$$\dot{\beta}_N = \begin{bmatrix} -(1 + \frac{L_N \mathrm{c}\beta_N}{L_{hN}}) & \frac{\mathrm{s}\beta_N}{L_{hN}} \end{bmatrix} \boldsymbol{u}_N, \quad (31)$$

*with equation (30) valid for* $i = 1, \ldots, N-1$, *and with matrix* $\boldsymbol{J}_B(\beta_{i+1}, \ldots, \beta_N) \triangleq \prod_{j=i+1}^{N} \boldsymbol{J}_j^{-1}(\beta_j)$ *in the form*

$$\boldsymbol{J}_B(\cdot) = \begin{bmatrix} r_{11}(\beta_{i+1}, \ldots, \beta_N) & r_{12}(\beta_{i+1}, \ldots, \beta_N) \\ r_{21}(\beta_{i+1}, \ldots, \beta_N) & r_{22}(\beta_{i+1}, \ldots, \beta_N) \end{bmatrix}. \quad (32)$$

*All the matrix entries* $r_{lk}(\beta_{i+1}, \ldots, \beta_N)$ *are the bounded and smooth functions resulting from the product of matrices* $\boldsymbol{J}_j^{-1}(\beta_j)$ *determined by (14). Application of (28) into (30) and (31) yields:*

$$\dot{\beta}_i = v_N \begin{bmatrix} -(1 + \frac{L_i \mathrm{c}\beta_i}{L_{hi}}) & \frac{\mathrm{s}\beta_i}{L_{hi}} \end{bmatrix} \begin{bmatrix} r_{12}(\beta_{i+1}, \ldots, \beta_N) \\ r_{22}(\beta_{i+1}, \ldots, \beta_N) \end{bmatrix},$$

$$\dot{\beta}_N = v_N \frac{\mathrm{s}\beta_N}{L_{hN}}.$$

---

[6]Generally defined by: $\|\boldsymbol{A}\| = \sqrt{\sum_{i,j} |a_{ij}|^2}$, see e.g. [23].

*By application of (29) with definition (16) into the above equations and by using the fact that* $\mathrm{sgn}(L_{hN}) \equiv \mathrm{sgn}(L_{hi})$ *for any* $i$ *(under assumption A2), one obtains the closed-loop joint-angle dynamics in the form*

$$\dot{\beta}_i = \frac{-\bar{v}_N}{|L_{hi}|} \mathrm{s}\beta_i \prod_{j=i+1}^{N} \mathrm{c}\beta_j + \Delta_i(\beta_i, \ldots, \beta_N), \quad (33)$$

$$\dot{\beta}_N = \frac{-\bar{v}_N}{|L_{hN}|} \mathrm{s}\beta_N, \quad (34)$$

*where*

$$\Delta_i(\beta_i, \ldots, \beta_N) = \delta_i(\beta_i, \ldots, \beta_N) + d_i(\beta_i, \ldots, \beta_N), \quad (35)$$

$$\delta_i(\cdot) = \frac{\bar{v}_N}{\mathrm{sgn}(L_{hi})} \left(1 + \frac{L_i \mathrm{c}\beta_i}{L_{hi}}\right) r_{12}(\beta_{i+1}, \ldots, \beta_N), \quad (36)$$

$$d_i(\cdot) = \frac{-\bar{v}_N \mathrm{s}\beta_i}{|L_{hi}|} r_{22}^*(\beta_{i+1}, \ldots, \beta_N). \quad (37)$$

*The term* $r_{22}^*(\beta_{i+1}, \ldots, \beta_N)$ *used in (37) results from equation*

$$r_{22}(\beta_{i+1}, \ldots, \beta_N) = \prod_{j=i+1}^{N} \mathrm{c}\beta_j + r_{22}^*(\beta_{i+1}, \ldots, \beta_N), \quad (38)$$

*which has been obtained by direct inspection of a form of product* $\prod_{j=i+1}^{N} \boldsymbol{J}_j^{-1}(\beta_j)$. *It can be easily checked that* $\bar{\boldsymbol{\beta}} = [\bar{\beta}_1 \ \ldots \ \bar{\beta}_N]^\top$ *with* $\bar{\beta}_i = 2k\pi$, $k = 0, \pm1, \ldots$, $i = 1, \ldots, N$ *belong to a set of equilibria of dynamics (33)-(34), since (according to (32), (91), and (38))* $r_{12}(\bar{\boldsymbol{\beta}}) = 0$, $r_{22}^*(\bar{\boldsymbol{\beta}}) = 0$, *and according to (35)-(37) also* $\Delta_i(\bar{\boldsymbol{\beta}}) = \delta_i(\bar{\boldsymbol{\beta}}) + d_i(\bar{\boldsymbol{\beta}}) = 0$ *for all* $i = 1, \ldots, N-1$. *Naturally, we are mainly interested in the special equilibrium* $\bar{\boldsymbol{\beta}} = \boldsymbol{0}$. *Let us analyze its local stability assuming that* $\boldsymbol{\beta}(0)$ *is sufficiently close to zero.*

*The form of equation (34) immediately allows concluding about local asymptotic stability of* $\bar{\beta}_N = 0$, *since the time-derivative of the positive definite function* $V_N(\beta_N) \triangleq (1 - \mathrm{c}\beta_N)$ *is negative definite*

$$\dot{V}_N = -\frac{\bar{v}_N}{|L_{hN}|}(\mathrm{s}\beta_N)^2 < 0 \quad (39)$$

*for all* $\beta_N$ *locally around* $\bar{\beta}_N = 0$.

*To show the asymptotic stability for the remaining dynamics represented by (33) for* $i = 1, \ldots, N-1$ *one estimates the upper bound of* $\Delta_i(\cdot)$ *as follows (cf. (35)):*

$$|\Delta_i(\cdot)| \le |\delta_i(\cdot)| + |d_i(\cdot)|, \quad (40)$$

*where (according to (36)-(37))*

$$|\delta_i(\cdot)| \le \bar{v}_N \left(1 + \frac{L_i}{|L_{hi}|}\right) |r_{12}(\cdot)|, \quad (41)$$

$$|d_i(\cdot)| \le \frac{\bar{v}_N}{|L_{hi}|} |r_{22}^*(\cdot)|. \quad (42)$$

*Let us define the positive definite function* $V_i(\beta_i) \triangleq (1 - \mathrm{c}\beta_i)$. *Its time-derivative takes the form (using notion*

$c\boldsymbol{\beta}_{i+1}^{N} := \prod_{j=i+1}^{N} c\beta_j$ for compactness):

$$\dot{V}_i = s\beta_i \dot{\beta}_i = -\frac{\bar{v}_N c\boldsymbol{\beta}_{i+1}^{N}}{|L_{hi}|} (s\beta_i)^2 + \Delta_i(\cdot)s\beta_i$$

$$\leq -\frac{\bar{v}_N c\boldsymbol{\beta}_{i+1}^{N}}{|L_{hi}|} (s\beta_i)^2 + |\Delta_i(\cdot)| |s\beta_i| + (\xi - \xi)(s\beta_i)^2$$

$$\leq -\left(\frac{\bar{v}_N c\boldsymbol{\beta}_{i+1}^{N}}{|L_{hi}|} - \xi\right)(s\beta_i)^2 + W(\beta_i, \ldots, \beta_N),$$

where $W(\beta_i, \ldots, \beta_N) = |s\beta_i|(|\Delta_i(\beta_i, \ldots, \beta_N)| - \xi|s\beta_i|)$ and $\xi$ is some function which has to be designed. To make the time-derivative $\dot{V}_i$ non-positive one proposes to choose

$$\xi \triangleq \frac{\bar{v}_N c\boldsymbol{\beta}_{i+1}^{N}}{|L_{hi}|}\bar{\xi}, \qquad \bar{\xi} \in (0, 1) \qquad (43)$$

simultaneously requiring that function $W(\beta_i, \ldots, \beta_N)$ is non-positive. It will be met for $|\Delta_i(\beta_i, \ldots, \beta_N)| \leq \xi|s\beta_i|$ which, after recalling (41), (42), and (43), leads to the following stability condition

$$|s\beta_i| \geq \frac{\bar{L}_i |r_{12}(\beta_{i+1}, \ldots, \beta_N)| + |r_{22}^*(\beta_{i+1}, \ldots, \beta_N)|}{\bar{\xi} \prod_{j=i+1}^{N} c\beta_j} \qquad (44)$$

with $\bar{L}_i = (|L_{hi}| + L_i)$. Let us consider when condition (44) may be met, and proceed the analysis by going back from the $(N-1)$-st joint to the first one. Let us take $i := N-1$. Since $\beta_N(t) \to 0$ (due to (39)) there exists a time instant $\bar{t}_N < \infty$ when $|\beta_N(t)| < \pi/2$ for all $t \geq \bar{t}_N$. Hence, $\prod_{j=N-1+1}^{N} c\beta_j \equiv c\beta_N$ is positive for all $t \geq \bar{t}_N$. Note also that for $i := N-1$ one has

$$r_{12}(\beta_N) = \frac{s\beta_N}{L_{hN}}, \qquad r_{22}^* \equiv 0, \qquad (45)$$

and $r_{12}(\beta_N) \to 0$ as $\beta_N \to 0$. Thus, there exists time instant $t_{N-1} < \infty$ such that for all $t \geq t_{N-1}$ inequality (44) is satisfied implying convergence $\beta_{N-1}(t) \to 0$ for $t \geq t_{N-1}$. Let us take $i := N-2$. Since $\beta_N(t), \beta_{N-1}(t) \to 0$, there exists a time instant $\bar{t}_{N-1} < \infty$ when $|\beta_N(t)| < \pi/2$ and $|\beta_{N-1}(t)| < \pi/2$ for all $t \geq \bar{t}_{N-1}$. Hence, $\prod_{j=N-2+1}^{N} c\beta_j \equiv c\beta_{N-1}c\beta_N$ is positive for all $t \geq \bar{t}_{N-1}$. Note also that for $i := N-2$ one has

$$r_{12}(\beta_{N-1}, \beta_N) = \frac{-L_{N-1}c\beta_{N-1}s\beta_N}{L_{hN-1}L_{hN}} + \frac{s\beta_{N-1}c\beta_N}{L_{hN-1}}, \quad (46)$$

$$r_{22}^*(\beta_{N-1}, \beta_N) = \frac{L_{N-1}s\beta_{N-1}s\beta_N}{L_{hN}}, \qquad (47)$$

and the above functions tend to zero as $\beta_N, \beta_{N-1} \to 0$. Thus, there exists time instant $t_{N-2} < \infty$ such that for all $t \geq t_{N-2}$ inequality (44) is satisfied implying convergence $\beta_{N-2}(t) \to 0$ for $t \geq t_{N-2}\ldots$Proceeding similar reasoning for all the remaining indexes $i$ from $N-3$ to $1$ one can conclude local asymptotic stability of the equilibrium $\bar{\boldsymbol{\beta}} = \mathbf{0}$ of joint-angle dynamics represented by (33)-(34): $\lim_{t\to\infty} \|\boldsymbol{\beta}(t)\| = 0$. The above result implies that by taking $\epsilon > 0$ in (29), there exists time instant $T < \infty$ such that $\|\boldsymbol{\beta}(T)\| \leq \epsilon$, and according to (29) the virtual control input $\boldsymbol{u}_N(T)$ is set to zero making the control input (27)

equal to zero, too. Due to the driftless nature of dynamics (30)-(31) all the joint angles are frozen for $t \geq T$ implying practical stability in the sense that $\forall t \geq T \ \|\boldsymbol{\beta}(t)\| \leq \epsilon$.

Worth to note that the above conclusions on stability and convergence remain valid for the whole set of equilibria $\bar{\boldsymbol{\beta}}$ with $\bar{\beta}_i = 2k\pi$, $k = 0, \pm 1, \ldots$ Convergence toward $\bar{\beta}_i = 2k\pi$ for $k \neq 0$ implies the vehicle folding effect, which usually should be avoided due to the presence of mechanical limitations in vehicle joints. Convergence to the point $\bar{\boldsymbol{\beta}} = \mathbf{0}$ (instead to $\bar{\boldsymbol{\beta}} = [2k\pi \ \ldots \ 2k\pi]^\top$ for $k \neq 0$) depends on the initial condition $\|\boldsymbol{\beta}(0)\|$ which should be sufficiently close to zero to avoid the folding phenomenon. Furthermore, the forms of functions (45)-(47) indicate that the values of hitching offsets may also influence appearance/avoidance of the folding effect. Longer hitching offsets of the following trailers make a numerator on the right-hand side of (44) smaller, hence the convergence condition (44) can be met earlier preventing substantial divergence of the $i$-th joint angle during a transient stage. $\square$

**Remark 1** *Application of (27)-(29) into (10) forces the last trailer motion with zero angular velocity and with a constant longitudinal velocity determined by (29), which has a constant sign within the whole control time-horizon. According to definitions (29) and (16) the sign of longitudinal velocity $v_N$ depends on the sign of hitching offsets used in a vehicle (cf. assumption A2). Hence, for $\sigma = 1$ one obtains the backward lining-up maneuvers, while for $\sigma = -1$ – the forward lining-up maneuvers. Furthermore, the form of (28) indicates that the last trailer preserves its initial orientation: $\forall t \geq 0 \ \theta_N(t) \equiv \theta_N(0)$. This side-effect seems to be beneficial in practical applications, because it allows anticipating motion of the last segment during the overall lining-up maneuver, and in a terminal stage also of the whole articulated vehicle. Obviously, since the posture $\boldsymbol{q}_N$ is controlled in an open loop its evolution is inherently non-robust to external disturbances.*

### 4.2 Passive lining-up strategy

The alternative passive lining-up strategy (well known from the practical experience) can be formulated by the following proposition.

**Proposition 2 (Passive lining-up)** *The open-loop control law*

$$\boldsymbol{u}_0 \triangleq \begin{bmatrix} \omega_0 \\ v_0 \end{bmatrix} \triangleq \begin{bmatrix} 0 \\ v_0 \end{bmatrix} \qquad (48)$$

*with*

$$v_0 \triangleq \begin{cases} \bar{v}_0 & for \quad \|\boldsymbol{\beta}\| > \epsilon \\ 0 & for \quad \|\boldsymbol{\beta}\| \leq \epsilon \end{cases}, \quad 0 < \bar{v}_0 < \infty \qquad (49)$$

*applied into kinematics (8) solves Problem 1 and will be called the passive lining-up strategy.*

**Proof 2** *The analysis will be performed by a strict analogy to the proof of Proposition 1.*

*According to the form of definitions (48)-(49) holds $\|\boldsymbol{u}_0\| \leq \bar{v}_0 < \infty$, thus the claim about boundedness of control input $\boldsymbol{u}_0$ is immediate in this case.*

Now, let us analyze stability of system (19) with open-loop control determined by (48)-(49). Recalling (20) and (21) one can rewrite dynamics (19) in the compact form

$$\dot{\beta}_1 = \left[1 + \frac{L_{h1}c\beta_1}{L_1} \quad \frac{-s\beta_1}{L_1}\right] \boldsymbol{u}_0, \tag{50}$$

$$\dot{\beta}_i = \left[1 + \frac{L_{hi}c\beta_i}{L_i} \quad \frac{-s\beta_i}{L_i}\right] \boldsymbol{J}_F(\beta_1,\ldots,\beta_{i-1})\boldsymbol{u}_0, \tag{51}$$

with equation (51) valid for $i = 2,\ldots,N$, and with matrix $\boldsymbol{J}_F(\beta_1,\ldots,\beta_{i-1}) \triangleq \prod_{j=i-1}^{1} \boldsymbol{J}_j(\beta_j)$ in the form

$$\boldsymbol{J}_F(\cdot) = \begin{bmatrix} p_{11}(\beta_1,\ldots,\beta_{i-1}) & p_{12}(\beta_1,\ldots,\beta_{i-1}) \\ p_{21}(\beta_1,\ldots,\beta_{i-1}) & p_{22}(\beta_1,\ldots,\beta_{i-1}) \end{bmatrix}. \tag{52}$$

All the matrix entries $p_{lk}(\beta_1,\ldots,\beta_{i-1})$ are the bounded and smooth functions resulting from the product of matrices $\boldsymbol{J}_j(\beta_j)$ determined by (5). By application of (48)-(49) into equations (50)-(51) one obtains the joint-angle dynamics in the form

$$\dot{\beta}_1 = \frac{-\bar{v}_0}{L_1} s\beta_1 \tag{53}$$

$$\dot{\beta}_i = \frac{-\bar{v}_0}{L_i} s\beta_i \prod_{j=i-1}^{1} c\beta_j + \tilde{\Delta}_i(\beta_1,\ldots,\beta_i), \tag{54}$$

where

$$\tilde{\Delta}_i(\beta_1,\ldots,\beta_i) = \tilde{\delta}_i(\beta_1,\ldots,\beta_i) + \tilde{d}_i(\beta_1,\ldots,\beta_i), \tag{55}$$

$$\tilde{\delta}_i(\cdot) = \bar{v}_0 \left(1 + \frac{L_{hi}c\beta_i}{L_i}\right) p_{12}(\beta_1,\ldots,\beta_{i-1}), \tag{56}$$

$$\tilde{d}_i(\cdot) = \frac{-\bar{v}_0 s\beta_i}{L_i} p_{22}^*(\beta_1,\ldots,\beta_{i-1}). \tag{57}$$

The term $p_{22}^*(\beta_1,\ldots,\beta_{i-1})$ used in (57) results from equation

$$p_{22}(\beta_1,\ldots,\beta_{i-1}) = \prod_{j=i-1}^{1} c\beta_j + p_{22}^*(\beta_1,\ldots,\beta_{i-1}), \tag{58}$$

which has been obtained by direct inspection of a form of product $\prod_{j=i-1}^{1} \boldsymbol{J}_j(\beta_j)$. It can be easily checked that $\bar{\boldsymbol{\beta}} = [\bar{\beta}_1 \ldots \bar{\beta}_N]^\top$ with $\bar{\beta}_i = 2k\pi$, $k = 0,\pm1,\ldots$, $i = 1,\ldots,N$ belong a set of equilibria of open-loop dynamics (53)-(54), since (according to (52), (90), and (58)) $p_{12}(\bar{\boldsymbol{\beta}}) = 0$, $p_{22}^*(\bar{\boldsymbol{\beta}}) = 0$, and according to (55)-(57) also $\tilde{\Delta}_i(\bar{\boldsymbol{\beta}}) = \tilde{\delta}_i(\bar{\boldsymbol{\beta}}) + \tilde{d}_i(\bar{\boldsymbol{\beta}}) = 0$ for all $i = 2,\ldots,N$. Again, we are mainly interested in equilibrium $\bar{\boldsymbol{\beta}} = \boldsymbol{0}$. Let us analyze its local stability assuming that $\boldsymbol{\beta}(0)$ is sufficiently close to zero.

Due to the form of (53), and since $L_i > 0$ for all $i = 1,\ldots,N$, one can immediately conclude local asymptotic stability of $\bar{\beta}_1 = 0$, since the time-derivative of the positive definite function $V_1(\beta_1) \triangleq (1 - c\beta_1)$ is negative definite

$$\dot{V}_1 = -\frac{\bar{v}_0}{L_1}(s\beta_1)^2 < 0 \tag{59}$$

for all $\beta_1$ locally around $\bar{\beta}_1 = 0$.

To analyze stability for dynamics represented by (54) for $i = 2,\ldots,N$ let us estimate the upper bound of $\tilde{\Delta}_i(\cdot)$ as follows (cf. (55)):

$$\left|\tilde{\Delta}_i(\cdot)\right| \leq \left|\tilde{\delta}_i(\cdot)\right| + \left|\tilde{d}_i(\cdot)\right|, \tag{60}$$

where (according to (56)-(57))

$$\left|\tilde{\delta}_i(\cdot)\right| \leq \bar{v}_0 \left(1 + \frac{|L_{hi}|}{L_i}\right) |p_{12}(\cdot)|, \tag{61}$$

$$\left|\tilde{d}_i(\cdot)\right| \leq \frac{\bar{v}_0}{L_i} |p_{22}^*(\cdot)|. \tag{62}$$

Defining the positive definite function $V_i(\beta_i) \triangleq (1 - c\beta_i)$, its time-derivative can be assessed as follows (using notion $c\boldsymbol{\beta}_{i-1}^1 := \prod_{j=i-1}^{1} c\beta_j$ for compactness):

$$\dot{V}_i = s\beta_i\dot{\beta}_i = -\frac{\bar{v}_0 c\boldsymbol{\beta}_{i-1}^1}{L_i}(s\beta_i)^2 + \tilde{\Delta}_i(\cdot)s\beta_i$$

$$\leq -\frac{\bar{v}_0 c\boldsymbol{\beta}_{i-1}^1}{L_i}(s\beta_i)^2 + \left|\tilde{\Delta}_i(\cdot)\right||s\beta_i| + (\tilde{\xi} - \tilde{\xi})(s\beta_i)^2$$

$$\leq -\left(\frac{\bar{v}_0 c\boldsymbol{\beta}_{i-1}^1}{L_i} - \xi\right)(s\beta_i)^2 + W(\beta_1,\ldots,\beta_i),$$

where $W(\beta_1,\ldots,\beta_i) = |s\beta_i|\left(\left|\tilde{\Delta}_i(\beta_1,\ldots,\beta_i)\right| - \tilde{\xi}|s\beta_i|\right)$ and $\tilde{\xi}$ is some function which has to be designed. To make the time-derivative $\dot{V}_i$ non-positive one proposes to choose

$$\tilde{\xi} \triangleq \frac{\bar{v}_0 c\boldsymbol{\beta}_{i-1}^1}{L_i}\bar{\xi}, \qquad \bar{\xi} \in (0,1) \tag{63}$$

simultaneously requiring that function $W(\beta_1,\ldots,\beta_i)$ is non-positive. It will be satisfied for $\left|\tilde{\Delta}_i(\beta_1,\ldots,\beta_i)\right| \leq \tilde{\xi}|s\beta_i|$ which, after recalling (61), (62), and (63), leads to the following stability condition

$$|s\beta_i| \geq \frac{\bar{L}_i |p_{12}(\beta_1,\ldots,\beta_{i-1})| + |p_{22}^*(\beta_1,\ldots,\beta_{i-1})|}{\bar{\xi} \prod_{j=i-1}^{1} c\beta_j} \tag{64}$$

with $\bar{L}_i = (|L_{hi}| + L_i)$. Let us consider when condition (64) can be met, and proceed the analysis from the second joint toward the last one. Let us take $i := 2$. Since $\beta_1(t) \to 0$ (due to (59)) there exists a time instant $\bar{t}_1 < \infty$ when $|\beta_1(t)| < \pi/2$ for all $t \geq \bar{t}_1$. Hence, $\prod_{j=2-1}^{1} c\beta_j \equiv c\beta_1$ is positive for all $t \geq \bar{t}_1$. Note also that for $i := 2$ one has

$$p_{12}(\beta_1) = \frac{s\beta_1}{L_1}, \qquad p_{22}^* \equiv 0, \tag{65}$$

and $p_{12}(\beta_1) \to 0$ as $\beta_1 \to 0$. Hence, there exists time instant $t_2 < \infty$ such that for all $t \geq t_2$ inequality (64) is satisfied implying convergence $\beta_2(t) \to 0$ for $t \geq t_2$. Let us take $i := 3$. Since $\beta_1(t), \beta_2(t) \to 0$ there exists a time instant $\bar{t}_2 < \infty$ when $|\beta_1(t)| < \pi/2$ and $|\beta_2(t)| < \pi/2$ for all $t \geq \bar{t}_2$. Hence, $\prod_{j=3-1}^{1} c\beta_j \equiv c\beta_2 c\beta_1$ is positive for all $t \geq \bar{t}_2$. Furthermore, for $i := 3$ hold

$$p_{12}(\beta_1,\beta_2) = \frac{-L_{h2}s\beta_1 c\beta_2}{L_1 L_2} + \frac{c\beta_1 s\beta_2}{L_2}, \tag{66}$$

$$p_{22}^*(\beta_1,\beta_2) = \frac{L_{h2}s\beta_1 s\beta_2}{L_1}, \tag{67}$$

and the above functions tend to zero as $\beta_1, \beta_2 \to 0$. Thus, there exists time instant $t_3 < \infty$ such that for all $t \geq t_3$ inequality (64) is satisfied implying convergence $\beta_3(t) \to$

0 *for* $t \geq t_3$... *Proceeding similar reasoning for all the remaining indexes $i$ from 4 to $N$ one can conclude local asymptotic stability of the equilibrium $\bar{\boldsymbol{\beta}} = \mathbf{0}$ of joint-angle dynamics (53)-(54):* $\lim_{t \to \infty} \| \boldsymbol{\beta}(t) \| = 0$. *According to the above result one can conclude that by taking $\epsilon > 0$ in (49) there exists time instant $T < \infty$ such that $\| \boldsymbol{\beta}(T) \| \leq \epsilon$, and according to (49) the control input $\mathbf{u}_0(T)$ is set to zero. Due to the driftless nature of dynamics (50)-(51) all the joint angles are* frozen *for $t \geq T$ implying practical stability in the sense that $\forall t \geq T \ \| \boldsymbol{\beta}(t) \| \leq \epsilon$.*

*The above conclusions on stability and convergence are valid for the whole set of equilibria $\bar{\boldsymbol{\beta}}$ with $\bar{\beta}_i = 2k\pi$, $k = 0, \pm 1, \ldots$ Similarly as for the active lining-up strategy convergence toward $\bar{\beta}_i = 2k\pi$ for $k \neq 0$ implies the* vehicle folding effect. *Convergence to the point $\bar{\boldsymbol{\beta}} = \mathbf{0}$ (instead to $\bar{\boldsymbol{\beta}} = [2k\pi \ \ldots \ 2k\pi]^\top$ for $k \neq 0$) depends on the initial condition $\| \boldsymbol{\beta}(0) \|$ which should be sufficiently close to zero to avoid the folding phenomenon. According to the forms of functions (65)-(67) one observes that the lengths of trailers may also influence appearance/avoidance of the folding effect, since the longer preceding trailers make a numerator on the right-hand side of (64) smaller. As a consequence, the convergence condition (64) can be met earlier preventing substantial divergence of the $i$-th joint angle during a transient stage.* $\square$

**Remark 2** *By recalling the form of (48) it is clear that the tractor segment preserves its initial orientation, however this side-effect is inherently non-robust since the tractor is controlled in the open loop. Furthermore, the sign of the longitudinal velocity $v_0$ is always non-negative, thus the passive lining-up maneuvers proposed above are always performed in the forward strategy. Moreover, in contrast to the active lining-up control, stability of the closed-loop system for the passive strategy is not influenced by any of the hitching offsets. Hence, stability and convergence results obtained for the passive strategy remain valid for any type of $N$-trailer vehicles (nSNT, GNT, and SNT).*

## 5 Quantitative studies and extensions

### 5.1 Quantitative analysis of joint-angle dynamics

Apart from the nonlinear analysis performed in the previous section, it is instructive to look at the linearized form of the joint angle dynamics for the two lining-up strategies.

In the case of the active lining-up strategy the joint-angle dynamics linearized around equilibrium $\bar{\boldsymbol{\beta}} = \mathbf{0}$ take the form

$$
\begin{bmatrix} \dot{\beta}_1 \\ \dot{\beta}_2 \\ \vdots \\ \dot{\beta}_i \\ \vdots \\ \dot{\beta}_N \end{bmatrix} = \underbrace{\begin{bmatrix} \gamma_{11} & \gamma_{12} & \ldots & \gamma_{1i} & \ldots & \gamma_{1N} \\ 0 & \gamma_{22} & \ldots & \gamma_{2i} & \ldots & \gamma_{2N} \\ \vdots & \vdots & \ddots & \vdots & \ldots & \vdots \\ 0 & 0 & \ldots & \gamma_{ii} & \ldots & \gamma_{iN} \\ \vdots & \vdots & \ldots & \vdots & \ddots & \vdots \\ 0 & 0 & \ldots & 0 & \ldots & \gamma_{NN} \end{bmatrix}}_{\boldsymbol{\Gamma}} \begin{bmatrix} \beta_1 \\ \beta_2 \\ \vdots \\ \beta_i \\ \vdots \\ \beta_N \end{bmatrix}, \quad (68)
$$

where $\boldsymbol{\Gamma}$ is the upper-triangular state-matrix, and for $i = 1, \ldots, N$ and $k = i+1, \ldots, N$ hold:

$$
\gamma_{ii} = \frac{-\bar{v}_N}{|L_{hi}|}, \tag{69}
$$

$$
\gamma_{ik} = (-1)^{k-i-1} \frac{\bar{v}_N}{|L_{hk}|} \left( 1 + \frac{L_i}{L_{hi}} \right) \prod_{j=i+1}^{k-1} \frac{L_j}{L_{hj}}. \tag{70}
$$

The above result can be obtained by direct computations based on dynamics (33)-(34) with the help of partial derivatives presented in Appendix 7.2. The main diagonal

$$
\mathrm{diag}(\boldsymbol{\Gamma}) = \left\{ \frac{-\bar{v}_N}{|L_{h1}|}, \frac{-\bar{v}_N}{|L_{h2}|}, \ldots, \frac{-\bar{v}_N}{|L_{hN}|} \right\} \tag{71}
$$

determines the set of eigenvalues of matrix $\boldsymbol{\Gamma}$. All the eigenvalues are (real) negative which confirms the local asymptotic stability of the joint-angle dynamics. Moreover, for a selected velocity $\bar{v}_N$ the locus of eigenvalues directly and solely depends on the lengths of hitching offsets. As a consequence, the convergence rate of joint angles in the active strategy depends on the longitudinal speed of the last trailer and inversely proportional on the lengths of hitching offsets used in a vehicle.

In the case of the passive lining-up strategy the joint-angle dynamics linearized around equilibrium $\bar{\boldsymbol{\beta}} = \mathbf{0}$ take the form

$$
\begin{bmatrix} \dot{\beta}_1 \\ \dot{\beta}_2 \\ \vdots \\ \dot{\beta}_i \\ \vdots \\ \dot{\beta}_N \end{bmatrix} = \underbrace{\begin{bmatrix} \tilde{\gamma}_{11} & 0 & \ldots & 0 & \ldots & 0 \\ \tilde{\gamma}_{21} & \tilde{\gamma}_{22} & \ldots & 0 & \ldots & 0 \\ \vdots & \vdots & \ddots & \vdots & \ldots & \vdots \\ \tilde{\gamma}_{i1} & \tilde{\gamma}_{i2} & \ldots & \tilde{\gamma}_{ii} & \ldots & 0 \\ \vdots & \vdots & \ldots & \vdots & \ddots & \vdots \\ \tilde{\gamma}_{N1} & \tilde{\gamma}_{N2} & \ldots & \tilde{\gamma}_{Ni} & \ldots & \tilde{\gamma}_{NN} \end{bmatrix}}_{\tilde{\boldsymbol{\Gamma}}} \begin{bmatrix} \beta_1 \\ \beta_2 \\ \vdots \\ \beta_i \\ \vdots \\ \beta_N \end{bmatrix}
$$

$$(72)$$

with $\tilde{\boldsymbol{\Gamma}}$ being the lower-triangular state-matrix where for $i = 1, \ldots, N$ and $k = 1, \ldots, i-1$

$$
\tilde{\gamma}_{ii} = \frac{-\bar{v}_0}{L_i}, \tag{73}
$$

$$
\tilde{\gamma}_{ik} = (-1)^{i-k-1} \frac{\bar{v}_0}{L_k} \left( 1 + \frac{L_{hi}}{L_i} \right) \prod_{j=k+1}^{i-1} \frac{L_{hj}}{L_j}. \tag{74}
$$

The above equations can be obtained by direct computations based on dynamics (53)-(54) with the help of partial derivatives presented in Appendix 7.2. The main diagonal

$$
\mathrm{diag}(\tilde{\boldsymbol{\Gamma}}) = \left\{ \frac{-\bar{v}_0}{L_1}, \frac{-\bar{v}_0}{L_2}, \ldots, \frac{-\bar{v}_0}{L_N} \right\} \tag{75}
$$

defines the set of eigenvalues of matrix $\tilde{\boldsymbol{\Gamma}}$. Also in this case all the eigenvalues are (real) negative confirming the local asymptotic stability result claimed in the previous section. Now, for a selected velocity $\bar{v}_0$ the locus of eigenvalues directly and solely depends on the lengths of trailers. As a consequence, the convergence rate of joint angles in the passive strategy depends on the longitudinal tractor speed and inversely proportional on the lengths of trailers.

In practice, where the lining-up maneuvers are executed under conditions of a limited motion space, the more important than convergence rate is the *convergence distance* which has to be passed to line-up a vehicle chain with the prescribed precision $\epsilon$. According to the lining-up policies proposed in the paper one can assess distances which have to be passed by the distinguished segments for particular lining-up strategies (the last trailer or the tractor segment).

For the active lining-up strategy the last joint angle evolves in time according to the equation (exact solution of (34))

$$\beta_N(t) = 2\arctan\left(\tan\frac{\beta_N(0)}{2} \cdot \exp\left(\frac{-\bar{v}_N}{|L_{hN}|}t\right)\right),$$

valid for $\beta_N \in [-\pi, \pi]$. Assuming a constant longitudinal velocity $\bar{v}_N$ the distance passed by the last trailer within time $t$ is $s_N(t) = s_N(0) + \bar{v}_N t$ (from now on one assumes $s_N(0) = 0$ without lack of generality). At time $t = T$, when the norm $\|\boldsymbol{\beta}(t = T)\|$ decreases to the prescribed threshold $\epsilon$, the distance $s_N(T) = \bar{v}_N T$, thus $T = s_N(T)/\bar{v}_N$, and

$$\beta_N(T) = 2\arctan\left(\tan\frac{\beta_N(0)}{2} \cdot \exp\left(\frac{-s_N(T)}{|L_{hN}|}\right)\right).$$

According to the above equation one can assess the distance traveled by the last trailer as

$$s_N(T) = |L_{hN}| \ln\left(\frac{\tan\frac{\beta_N(0)}{2}}{\tan\frac{\beta_N(T)}{2}}\right), \qquad (76)$$

which is finite for $|\beta_N(0)| < \pi$ and $\epsilon > 0$. Note that distance (76) does not depend on velocity $\bar{v}_N$, but it proportionally depends on the length of hitching offset $|L_{hN}|$. Obviously, the exact value of $s_N(T)$ depends on the time horizon $T$ which results from initial condition $\|\boldsymbol{\beta}(0)\|$, prescribed precision $\epsilon$, and from the convergence rate of remaining angles $\beta_{N-1}(t), \ldots, \beta_1(t)$, which in turn (in view of (71)) depends on the remaining hitching offsets $L_{hN-1}$ to $L_{h1}$ and on $\bar{v}_N$. However, since the parameter $\bar{v}_N$ appears in all the elements of matrix $\boldsymbol{\Gamma}$ (cf. (69)-(70)) its effect preserves temporal relations between all the state variables (the same conclusion results directly from the driftless nature of original dynamics (24) together with the form of (28)). Hence, independently on the value of $\bar{v}_N$ the terminal value $\beta_N(T)$ must be unique (for fixed initial condition $\|\boldsymbol{\beta}(0)\|$) making the distance (76) invariant with respect to $\bar{v}_N$.

A similar analysis can be performed for the passive strategy but in this case by using dynamics of the first joint angle. The exact solution of (53) gives

$$\beta_1(t) = 2\arctan\left(\tan\frac{\beta_1(0)}{2} \cdot \exp\left(\frac{-\bar{v}_0}{L_1}t\right)\right),$$

which is valid for $\beta_1 \in [-\pi, \pi]$. Assuming constant longitudinal velocity $\bar{v}_0$ and $s_0(0) = 0$, the distance which is passed by the tractor at time $t = T$ is equal to $s_0(T) = \bar{v}_0 T$, thus $T = s_0(T)/\bar{v}_0$, and

$$\beta_1(T) = 2\arctan\left(\tan\frac{\beta_1(0)}{2} \cdot \exp\left(\frac{-s_0(T)}{L_1}\right)\right).$$

According to the above equation one can assess the distance traveled by the tractor

$$s_0(T) = L_1 \ln\left(\frac{\tan\frac{\beta_1(0)}{2}}{\tan\frac{\beta_1(T)}{2}}\right), \qquad (77)$$

which is finite for $|\beta_1(0)| < \pi$ and $\epsilon > 0$. Note that distance (77) does not depend on velocity $\bar{v}_0$, but it proportionally depends on the length $L_1$ of the first trailer. The exact value of $s_1(T)$ depends on the time horizon $T$, which results from initial condition $\|\boldsymbol{\beta}(0)\|$, prescribed precision $\epsilon$, and from the convergence rate of remaining angles $\beta_2(t), \ldots, \beta_N(t)$ which (in view of (75)) depends in turn on the lengths $L_2$ to $L_N$ of the remaining trailers and on $\bar{v}_0$. Since the parameter $\bar{v}_0$ appears in all the elements of matrix $\tilde{\boldsymbol{\Gamma}}$ (cf. (73)-(74)) its effect preserves temporal relations between all the state variables (the same conclusion results directly from the driftless nature of original dynamics (19) together with the form of (48)). Hence, independently on the value of $\bar{v}_0$ the terminal value $\beta_1(T)$ must be unique (for fixed initial condition $\|\boldsymbol{\beta}(0)\|$) making the distance (77) invariant to $\bar{v}_0$.

One may conclude the above quantitative considerations by the following general corollary.

**Corollary 1** *For the proposed lining-up strategies:*

C1. *the local convergence rate of particular joint angles depends proportionally on the longitudinal velocity applied to the distinguished segment and inversely proportionally on the vehicle kinematic parameters (on hitching offsets for the active lining-up, and on trailer lengths for the passive lining-up),*

C2. *distances passed by the distinguished segments do not depend on their longitudinal velocities, but they directly depend on the vehicle kinematic parameters (on hitching offsets for the active lining-up, and on trailer lengths for the passive lining-up).*

## 5.2 Applicability of lining-up strategies into GNT and SNT vehicles

Lining-up control strategies presented in Section 4 have been formulated under assumptions A1-A2 (see Section 2.2). In fact, only the active lining-up strategy requires satisfaction of assumptions A1-A2, because it utilizes the inverse transformation matrices (14) (well determined only for non-zero hitching offsets), and the common sign of hitching offsets in definition of control law (29). On the other hand, it is well known from practical experience (cf. Remark 2) that the passive lining-up strategy is valid for all types of N-trailers (nSNT, GNT, and SNT) with arbitrary (and possibly different) signs of particular hitching offsets. Therefore, extensions will be considered only with respect to the active lining-up strategy.

Let us repeal assumption A1 (still keeping A2). As a consequence, one admits that some or even all the joints in a vehicle are of on-axle type. Let us consider the $i$-th joint for which $L_{hi} = 0$. In this case one proposes two

different ways of replacing the ill-conditioned inverse relation (13), used then in definition (27), by an alternative well-determined transformation.

In the first approach one can approximate the transformation matrix (5) by defining

$$\hat{\boldsymbol{J}}_i(\beta_i, \varepsilon_i) \triangleq \begin{bmatrix} -\frac{\varepsilon_i}{L_i}\mathrm{c}\beta_i & \frac{1}{L_i}\mathrm{s}\beta_i \\ \varepsilon_i\mathrm{s}\beta_i & \mathrm{c}\beta_i \end{bmatrix}, \quad \varepsilon_i \neq 0 \qquad (78)$$

where $\varepsilon_i$ is a prescribed sufficiently small non-zero parameter. It is clear that $\hat{\boldsymbol{J}}_i(\beta_i, \varepsilon_i = 0) \equiv \boldsymbol{J}_i(\beta_i)$. However, by approximation (78) the inverse matrix

$$\hat{\boldsymbol{J}}_i^{-1}(\beta_i, \varepsilon_i) = \begin{bmatrix} -\frac{L_i}{\varepsilon_i}\mathrm{c}\beta_i & \frac{1}{\varepsilon_i}\mathrm{s}\beta_i \\ L_i\mathrm{s}\beta_i & \mathrm{c}\beta_i \end{bmatrix} \qquad (79)$$

is well determined. It allows application of the active lining-up controller (27)-(29) also to vehicles with on-axle joints by replacing the unbounded inverse matrices in (27) with their bounded approximations (79). Since one still should keep assumption A2, all the parameters $\epsilon_i$ have to meet relation

$$\forall i \geq 1 \quad \mathrm{sgn}(\epsilon_i) = \sigma, \qquad (80)$$

where $\sigma$ (cf. (16)) determines a common sign of all the non-zero hitching offsets present in a vehicle (in case of SNT vehicles, the common sign for all the parameters $\varepsilon_i$ can be chosen arbitrarily[7]). Note that a value of parameter $\varepsilon_i$ influences sensitivity of the closed loop system to noises present in measurements of joint angles, because $\varepsilon_i$ is placed in a denominator of particular elements in matrix (79). Hence, selection of $\varepsilon_i$ should result from a compromise between precision of approximation (79) and noise-sensitivity of a resultant closed-loop system.

The second approach to the ill-conditioned inverse relation (13) is to replace it with a transformation specialized for on-axle joints. An exemplary transformation has been introduced in [14] for N-trailers with on-axle hitching. In this approach the tractor input $\boldsymbol{u}_0(\boldsymbol{\beta}) \triangleq \boldsymbol{u}_{0d}(\boldsymbol{\beta})$, where the desired input $\boldsymbol{u}_{0d}(\boldsymbol{\beta})$ results from combination of velocity transformations specialized for particular types of vehicle joints. Desired control input for the last segment $\boldsymbol{u}_{Nd} = [\omega_{Nd}\ v_{Nd}]^\top$ is determined by definitions (28)-(29). For every off-axle joint the transformation is determined, by analogy to (13), as $\boldsymbol{u}_{i-1d} = \boldsymbol{J}_i^{-1}(\beta_i)\boldsymbol{u}_{id}$. However, for on-axle joint the ill-conditioned transformation is replaced with a mapping

$$\boldsymbol{u}_{i-1d} = \begin{bmatrix} \omega_{i-1d} \\ v_{i-1d} \end{bmatrix} = \boldsymbol{\Psi}_i(\beta_i, \boldsymbol{u}_{id}), \qquad (81)$$

where

$$\boldsymbol{\Psi}_i(\beta_i, \boldsymbol{u}_{id}) \triangleq \begin{bmatrix} \omega_{id} + k_i(\beta_{id} - \beta_i) \\ -\sigma\,|L_i\omega_{id}\mathrm{s}\beta_i + v_{id}\mathrm{c}\beta_i| \end{bmatrix}, \ k_i > 0, \quad (82)$$

and

$$\boldsymbol{u}_{id} = \begin{cases} \boldsymbol{\Psi}_{i+1}(\beta_{i+1}, \boldsymbol{u}_{i+1d}) & \text{if } (i+1)\text{-st joint} \quad \text{is on-axle,} \\ \boldsymbol{J}_{i+1}^{-1}(\beta_{i+1})\boldsymbol{u}_{i+1d} & \text{if } (i+1)\text{-st joint} \quad \text{is off-axle.} \end{cases}$$

[7]According to the desired motion strategy of a vehicle (backward/forward).

In definition (82) the term

$$\beta_{id} \triangleq \mathrm{Atan2c}\,(-\sigma\,L_i\omega_{id}, -\sigma\,v_{id}) \in \mathbb{R} \qquad (83)$$

is a desired joint-angle, $k_i$ is a design coefficient, and $\mathrm{Atan2c}\,(\cdot, \cdot) : \mathbb{R} \times \mathbb{R} \mapsto \mathbb{R}$ is a continuous version of the four-quadrant inverse tangent function $\mathrm{Atan2}\,(\cdot, \cdot) : \mathbb{R} \times \mathbb{R} \mapsto [-\pi, \pi)$ (see [18]). In the first row of definition (82) a simple proportional control law for the $i$-th joint angle has been included in the form of component $k_i(\beta_{id} - \beta_i)$. Application of mapping (81) with a sufficiently high coefficient $k_i$ makes angle $\beta_i$ of the on-axle joint convergent toward $\beta_{id}$. Since (83) tends to zero in time (as a direct consequence of the lining-up effect in the $(i+1)$-st joint) or it is equal to zero for $i = N$ (by definitions (28)-(29)) the lining-up phenomenon can be obtained also for the on-axle joint.

Effectiveness of the two alternative approaches determined by matrix (79) and mapping (81) will be examined in Section 6.2.

Finally, let us note a special case, where the active lining-up strategy can be applied despite violation of assumption A2. Suppose a vehicle consists of two sub-chains of segments, where the first $l$ joints ($l < N$) have the non-positive hitching offsets, while the remaining $N - l$ hitching offsets are arbitrary. Treating the $l$-th trailer as a distinguished vehicle segment, one can apply the lining-up strategy by taking $\boldsymbol{u}_l$ instead of $\boldsymbol{u}_N$ in (27) and defining $\boldsymbol{u}_l$ according to (28)-(29) with $\sigma = -1$. As a consequence, the forward active lining-up strategy can be forced for the first sub-chain of segments, allowing the remaining $N - l$ joint angles terminally tend to zero through the passive lining-up process (in this case the $l$-th segment can be treated as a forward-moving tractor for the second sub-chain of a vehicle). Of course, all the consequences resulting from the active lining-up maneuvers concern in this case only the first sub-chain of a vehicle.

# 6 Numerical and experimental validation

Performance of the proposed lining-up strategies has been verified with 3-trailer kinematics ($N = 3$). Simulations have been conducted for nSNT vehicles (satisfying assumptions A1-A2), while experimental tests have been conducted for nSNT as well as for GNT and SNT kinematics (repealing assumption A1).

## 6.1 Numerical simulations

Results of two exemplary simulations, S1 and S2, presenting performance of the active lining-up control have been presented in Figs. 2-3. The X-Y plots illustrate initial (denoted by $\boldsymbol{q}(0)$) and final configurations of the vehicle. In both cases the following initial conditions and parameters have been selected: $\beta_i(0) = (-1)^i \cdot \frac{\pi}{3}$, $\epsilon = 0.001\,\mathrm{rad}$, $\bar{v}_3 = 0.2\,\mathrm{m/s}$. Simulation S1 presents backward lining-up maneuvers obtained for positive hitching offsets $L_{hi} = 0.1\,\mathrm{m}$ and trailer lengths $L_i = 0.15\,\mathrm{m}$ ($i = 1, 2, 3$). Simulation S2 presents forward lining-up
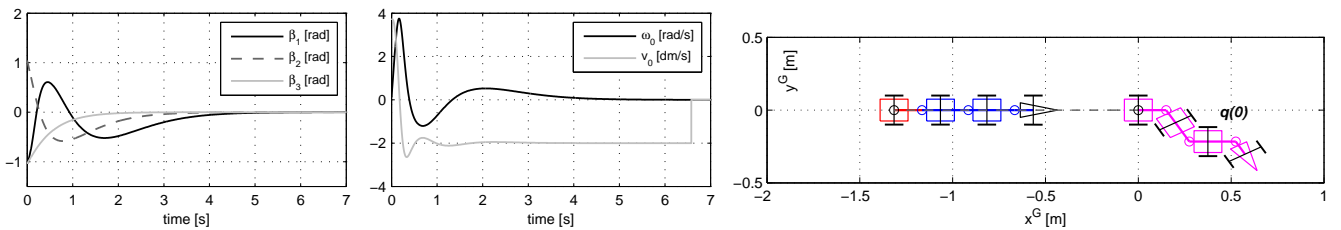
**Figure 2:** S1: simulation results of active lining-up maneuvers for $L_{hi} > 0$ ($q(0)$ indicates the initial vehicle configuration highlighted in magenta)
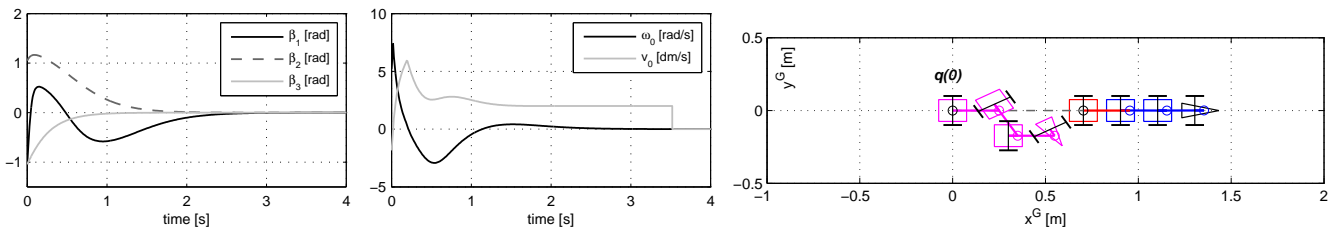


**Figure 3:** S2: simulation results of active lining-up maneuvers for $L_{hi} < 0$ ($q(0)$ indicates the initial vehicle configuration highlighted in magenta)

maneuvers for negative offsets $L_{hi} = -0.05\,\text{m}$ and trailer lengths $L_i = 0.25\,\text{m}$. The following distances $s_3(T_a)$ passed by the last trailer, and convergence time-horizons $T_a$ have been obtained for particular simulations (compared in brackets with corresponding values of $s_0(T_p)$ and $T_p$, respectively, obtained for passive lining-up maneuvers) – for S1: $s_3(T_a) = 1.316\,\text{m}$ ($s_0(T_p) = 1.828\,\text{m}$), $T_a = 6.578\,\text{s}$ ($T_p = 9.138\,\text{s}$), and for S2: $s_3(T_a) = 0.704\,\text{m}$ ($s_0(T_p) = 2.602\,\text{m}$), $T_a = 3.521\,\text{s}$ ($T_p = 13.01\,\text{s}$). One can observe that in considered cases effectiveness of the active lining-up maneuvers is substantially better in comparison to the passive ones. It is a direct consequence of the parameter ratio $|L_{hi}|/L_i$ which in the two simulations, S1 and S2, is less than unity.

More quantitative insight can be inferred from the exemplary (but representative) data collected in Table 1, where effectiveness of active and passive lining-up strategies has been compared as a function of the vehicle parameter ratio $L_{hi}/L_i$ for $L_{hi} > 0$. Particular values in Table 1 have been obtained using $\bar{v}_0 = \bar{v}_3 = 0.2\,\text{m/s}$, $\epsilon = 0.001\,\text{rad}$, $L_i = 0.15\,\text{m}$, and taking $\beta_i(0) = (-1)^i \cdot \frac{\pi}{3}$ ($i = 1, 2, 3$). Values of cost functionals

$$J_{0a} \triangleq \int_0^{T_a} \| \boldsymbol{u}_0(t) \|^2\, dt, \quad J_{0p} \triangleq \int_0^{T_p} \| \boldsymbol{u}_0(t) \|^2\, dt, \quad (84)$$

$$J_{3a} \triangleq \int_0^{T_a} \| \boldsymbol{u}_3(t) \|^2\, dt, \quad J_{3p} \triangleq \int_0^{T_p} \| \boldsymbol{u}_3(t) \|^2\, dt, \quad (85)$$

have been computed, where $\boldsymbol{u}_0 = [\omega_0 \ v_0]^\top$ is the tractor input vector, and $\boldsymbol{u}_3 = [\omega_3 \ v_3]^\top$ is a velocity vector of the last trailer (treated here as a virtual control input for the active strategy). Functionals (84)-(85) represent the *control costs* for particular lining-up strategies related to the respective distinguished segments (the tractor-segment – numbered by 0, and the last trailer – numbered by 3).

Upon the data from Table 1 one can formulate several practical inferences. First, one observes that the active strategy becomes more effective than passive one for

$\frac{|L_{hi}|}{L_i} < 1$. Effectiveness means here a shorter distance which the distinguished segment has to pass during the lining-up maneuvers. It can be observed by analyzing the last column of Table 1, where ratio $\frac{s_3(T_a)}{s_0(T_p)}$ becomes less then unity for $\frac{L_{hi}}{L_i} < 1$. Slightly nonlinear relation between the parameter-ratio and distance-ratio has been illustrated in Figure 4. Second, for $\frac{L_{hi}}{L_i} = 1$ one observes
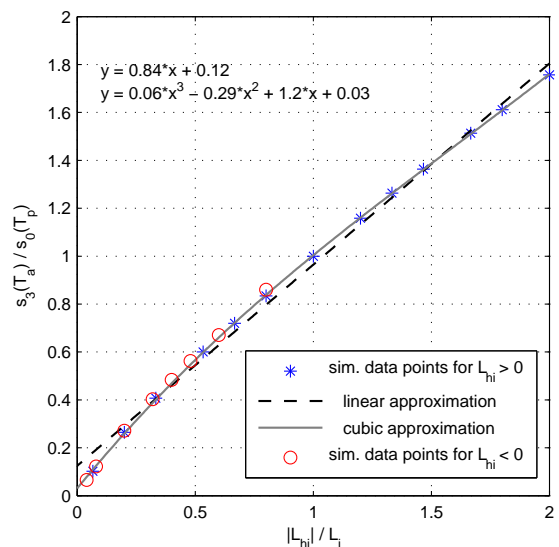


**Figure 4:** Quantitative dependence of the distance ratio $s_3(T_a)/s_0(T_p)$ on the vehicle parameter ratio $|L_{hi}|/L_i$ obtained for nSNT kinematics with $L_i = 0.15\,\text{m}$ and $L_{hi} > 0$ (star marks) and $L_{hi} < 0$ (circle marks), $i = 1, 2, 3$ (star-mark points taken from Table 1); linear and cubic approximations have been computed only upon star-mark points. Note that in case $L_{hi} < 0$ the range for $\frac{|L_{hi}|}{L_i} \geq 1$ seems to be impractical or even mechanically unfeasible, thus it has not been considered on the plot

the full equivalence between the two strategies which can be assessed looking at the highlighted row in the table. In this case not only distances $s_3(T_a)$ and $s_0(T_p)$ but also convergence times $T_a$ and $T_p$ are equivalent. Third, one can find substantial increase in convergence time $T_a$ and

11

Table 1: Quantitative comparison of active and passive lining-up maneuvers with respect to the parameter ratio $|L_{hi}|/L_i$ (values obtained for $L_i = 0.15$ m and $L_{hi} > 0$, $i = 1, 2, 3$)

| $L_{hi}$ [m] | $|L_{hi}|/L_i$ | $T_a$ [s] | $s_3(T_a)$ [m] | $J_{0a}$ | $J_{3a}$ | $T_p$ [s] | $s_0(T_p)$ [m] | $J_{0p}$ | $J_{3p}$ | $s_3(T_a)/s_0(T_p)$ |
|---|---|---|---|---|---|---|---|---|---|---|
| 0.01 | 0.067 | 0.850 | 0.170 | 4863.0 | 0.034 | 8.315 | 1.663 | 0.333 | 0.617 | 0.102 |
| 0.03 | 0.200 | 2.262 | 0.452 | 222.3 | 0.090 | 8.534 | 1.707 | 0.341 | 0.615 | 0.265 |
| 0.05 | 0.333 | 3.555 | 0.711 | 45.42 | 0.142 | 8.728 | 1.746 | 0.349 | 0.623 | 0.407 |
| 0.08 | 0.533 | 5.391 | 1.078 | 8.318 | 0.216 | 8.981 | 1.796 | 0.359 | 0.668 | 0.600 |
| 0.10 | 0.667 | 6.577 | 1.315 | 3.561 | 0.263 | 9.134 | 1.827 | 0.365 | 0.731 | 0.720 |
| 0.12 | 0.800 | 7.737 | 1.547 | 1.912 | 0.310 | 9.275 | 1.855 | 0.371 | 0.835 | 0.834 |
| **0.15** | **1.000** | **9.468** | **1.894** | **1.095** | **0.379** | **9.468** | **1.894** | **0.379** | **1.095** | **1.000** |
| 0.18 | 1.200 | 11.16 | 2.233 | 0.852 | 0.447 | 9.636 | 1.927 | 0.385 | 1.526 | 1.159 |
| 0.20 | 1.333 | 12.30 | 2.460 | 0.795 | 0.492 | 9.739 | 1.948 | 0.390 | 1.934 | 1.263 |
| 0.22 | 1.467 | 13.42 | 2.683 | 0.773 | 0.537 | 9.838 | 1.968 | 0.394 | 2.452 | 1.363 |
| 0.25 | 1.667 | 15.10 | 3.020 | 0.777 | 0.604 | 9.979 | 1.996 | 0.399 | 3.447 | 1.513 |
| 0.27 | 1.800 | 16.22 | 3.244 | 0.792 | 0.649 | 10.07 | 2.013 | 0.403 | 4.258 | 1.612 |
| 0.30 | 2.000 | 17.89 | 3.578 | 0.825 | 0.716 | 10.18 | 2.037 | 0.407 | 5.684 | 1.757 |

distance $s_3(T_a)$ for increasing hitching offsets $L_{hi} > L_i$, while the increase in time $T_p$ and distance $s_0(T_p)$ is rather slight. This tendency stays in agreement with theoretical linearized models (68)-(70) and (72)-(74), where the hitching offsets directly affect the convergence rate of the active lining-up process, while they influence passive maneuvers only by forms of the off-diagonal elements (74).

Finally, it is interesting to analyze the values of cost functionals. The tractor control cost $J_{0a}$ dramatically increases for very small offsets $L_{hi}$. The reason are very high values of elements of inverse matrices (14) used in propagation formula (15) – by decreasing $L_{hi}$ the propagation singularity is approached. As a consequence, one can observe large values of the tractor angular velocity. In contrast, the cost of the last-trailer inputs, $J_{3a}$, changes only slightly with ratio $L_{hi}/L_i$ indicating smooth behavior of the last segment during the active lining-up process. On the other hand, for the passive lining-up strategy one observes substantial increase in the cost $J_{3p}$ for $L_{hi} > L_i$. It reveals oscillatory behavior of the last trailer for substantially long hitching offsets. This effect is probably a consequence of the non-minimum-phase property of the N-trailers equipped with off-axle interconnections (oscillatory phenomena related to the non-minimum-phase property of N-trailers have been studied in [17]). Graphical illustration of trends of particular cost functionals has been provided in Fig. 5. Worth to note that functionals $J_{0a}$ with $J_{3p}$ and $J_{0p}$ with $J_{3a}$ intersect at a symmetry-point for $\frac{L_{hi}}{L_i} = 1$.

Figure 6 validates corollary C2 by showing the invariance of distance $s_3(T)$ (passed by the last trailer during active lining-up maneuvers) with respect to a longitudinal speed for three distinct values of $\bar{v}_3$. One observes that the only differences between the plots result from different convergence rates obtained for particular velocities, but in all cases final distance $s_3(T)$ is preserved. Similar results can be presented for the passive strategy showing that distance $s_0(T)$ is independent on velocity $\bar{v}_0$.

The last simulation example explains the locality of the convergence results proved in Section 4. Three plots presented in Fig. 7 show convergence of joint-angles for
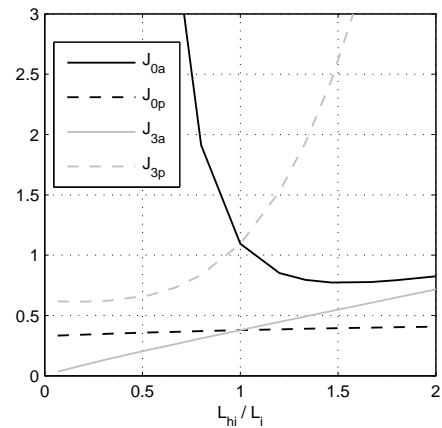


Figure 5: Plots of cost functionals (84)-(85) with respect to the parameter ratio $L_{hi}/L_i$ for values taken from Table 1
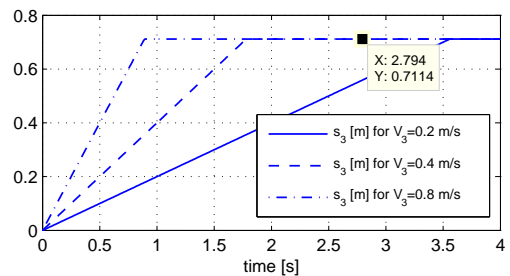


Figure 6: Invariance of a distance $s_3(T)$ passed by the last trailer with respect to the value of longitudinal velocity $\bar{v}_3 := V_3 > 0$ (plots for active lining-up maneuvers)

different values of positive hitching offsets in the case where initial conditions $\beta_i(0)$ are substantially far from zero-equilibrium (values $\beta_i(0) = (-1)^{i+1} \cdot \frac{\pi}{2}$, and parameters $L_i = 0.15$ m have been selected). One can see that for small hitching offsets the joint-angles can reach values even close to $\pm\pi$ (like for the first joint in Fig. 7B). For small hitching offsets ($L_{hi} = 0.05$ m in Fig. 7C) the first joint-angle passes value $\pi$ and converges toward the next stable equilibrium $\bar{\beta}_1 = 2\pi$ instead toward the zero-equilibrium. This phenomenon is called the *folding effect* and is rather undesirable in practical applications due
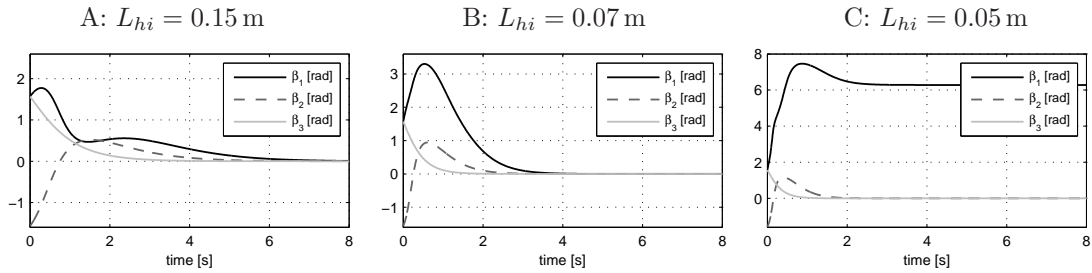
A: $L_{hi} = 0.15\,\text{m}$          B: $L_{hi} = 0.07\,\text{m}$          C: $L_{hi} = 0.05\,\text{m}$

**Figure 7:** Influence of hitching offset lengths on the convergence of joint-angles in the case where initial conditions are far from zero-equilibrium (selected values: $|\beta_i(0)| = \frac{\pi}{2}$ and $L_i = 0.15\,\text{m}$, $i = 1, 2, 3$)

to mechanical limitations usually present in the vehicle joints. Similar effect can be shown for passive lining-up maneuvers by choosing $L_i \ll L_{hi}$, $L_{hi} > 0$, and initial conditions sufficiently far from the zero-equilibrium.

## 6.2 Experimental results

The proposed lining-up strategies have been validated with the laboratory-scale RMP experimental vehicle presented in Fig. 8. The vehicle consists of a differentially driven tractor, three trailers of lengths $L_i = 0.229\,\text{m}$, $i = 1, 2, 3$, and joints with adjustable hitching offsets. Joint-angles are measured by 14-bit absolute encoders. Kinematic parameters of the tractor $b = 0.15\,\text{m}$, $r = 0.0293\,\text{m}$ denote the wheel base and the wheel radius, respectively (cf. Fig. 1). An auxiliary vision system (located out of the vehicle and mounted above a motion plane) allows estimating a posture of the last trailer upon a view of a LED marker attached to the last segment (posture measurements are used only in order to illustrate evolution of the vehicle configuration, and to verify the orientation invariance property for a distinguished segment). A block scheme presented in Fig. 9 explains a structure of the control and measurement subsystems implemented on the experimental testbed. The Velocity Scaling Block (VSB) denoted in Fig. 9, represents the scaling procedure which allows one to take into account control input limitations of the tractor resulting from the maximal admissible angular velocity $\omega_{w\,\text{max}} > 0$ of the tractor wheels. Denoting



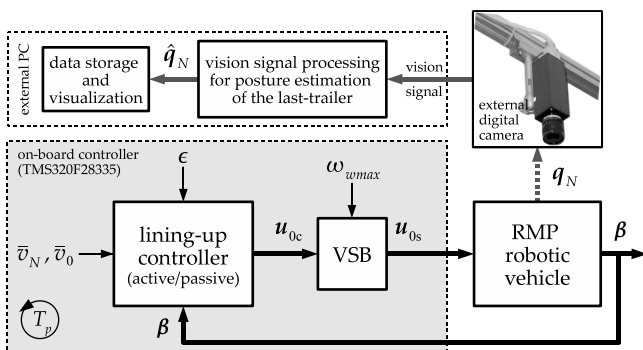**Figure 9:** Scheme of the lining-up control system with an external measurement vision system (control sampling time $T_p = 0.01\,\text{s}$)

by $\boldsymbol{u}_{0c} = [\omega_{0c}\ v_{0c}]^\top$ the nominal control input computed according to one of the proposed lining-up control laws,

the scaling procedure is determined by equation

$$\boldsymbol{u}_{0s}(t) \triangleq \frac{1}{s(t)}\,\boldsymbol{u}_{0c}(t), \qquad (86)$$

where

$$s(t) \triangleq \max\left\{1;\ \frac{|\omega_{0Rc}(t)|}{\omega_{w\,\text{max}}};\ \frac{|\omega_{0Lc}(t)|}{\omega_{w\,\text{max}}}\right\} \geq 1, \qquad (87)$$

is a strictly positive scaling function, and

$$\begin{bmatrix} \omega_{0Rc}(t) \\ \omega_{0Lc}(t) \end{bmatrix} = \begin{bmatrix} \frac{b}{2r} & \frac{1}{r} \\ -\frac{b}{2r} & \frac{1}{r} \end{bmatrix} \boldsymbol{u}_{0c}(t)$$

with $b$ and $r$ being the tractor wheel base and tractor wheel radius, respectively.

Numerous experiments have been conducted for active and passive lining-up maneuvers. Four selected sets of results for the active lining-up strategy are provided in Figs. 10-13. The results have been obtained by using the following common values of parameters: $\bar{v}_3 = 0.05\,\text{m/s}$, $\epsilon = 0.04\,\text{rad}$, and $\omega_{w\,\text{max}} = 3\,\text{rad/s}$. For convenience, an initial configuration $\boldsymbol{q}_3(0)$ of the last trailer was set to zero in all considered cases.

Experiment E1 illustrates performance for the nSNT vehicle with positive hitching offsets: $L_{h1} = 0.032\,\text{m}$, $L_{h2} = 0.048\,\text{m}$, and $L_{h3} = 0.040\,\text{m}$. Upon Fig. 10 one observes smooth maneuvers with preservation of an initial orientation for the last trailer ($\theta_3(0) \approx \theta_3(T_a)$). Lining-up time-horizon and distance passed by the last segment have been assessed, respectively, as $T_a \approx 21.05\,\text{s}$, and $s_3(T_a) \approx 0.478\,\text{m}$.

Application of the active lining-up strategy into the GNT and SNT vehicles has been examined for approximation (79) by the next two experiments – E2 and E3.

Experiment E2 shows the lining-up strategy for the GNT vehicle with $L_{h1} = L_{h3} = 0.0$, and $L_{h2} = 0.048\,\text{m}$. Since the two offsets are equal to zero, approximation (79) was applied taking $\varepsilon_1 = 0.016\,\text{m}$ and $\varepsilon_3 = 0.008\,\text{m}$. Fig. 11 illustrates successful maneuvers despite the mentioned approximation. However, a slight oscillatory behavior of the tractor can be observed in the terminal part of a control process together with a violation of the orientation invariance property for the last trailer ($\theta_3(T_a) \approx -4.5\,\text{deg}$). Lining-up time-horizon and distance passed by the last segment have been assessed, respectively, as $T_a \approx 23.11\,\text{s}$, and $s_3(T_a) \approx 0.184\,\text{m}$ (the distance does not include a small movement along $y^G$ axis).
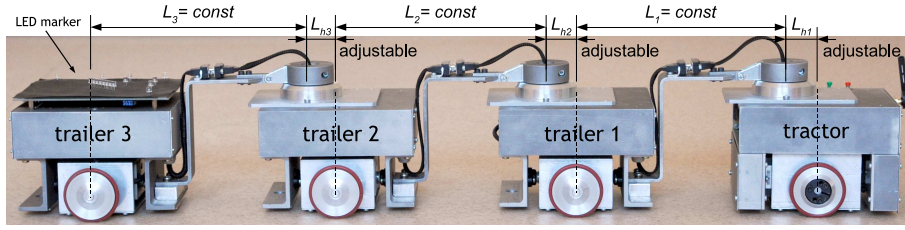
13

Figure 8: Experimental RMP 3-trailer robotic vehicle with adjustable hitching offsets
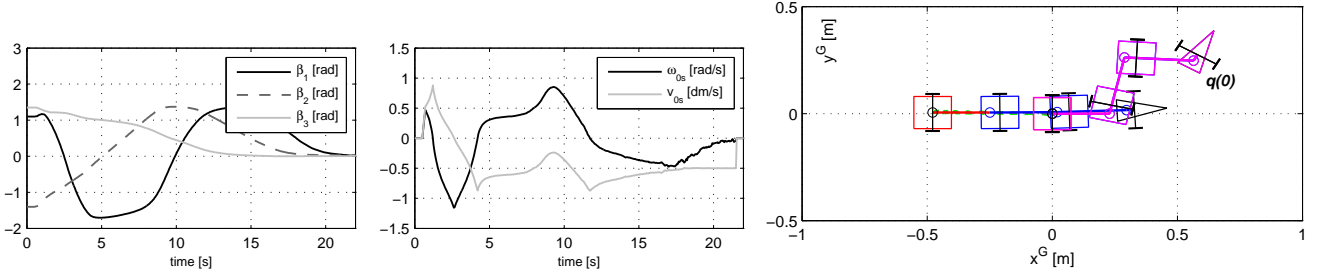


Figure 10: E1: experimental results of active lining-up maneuvers for nSNT vehicle ($q(0)$ indicates the initial vehicle configuration highlighted in magenta)
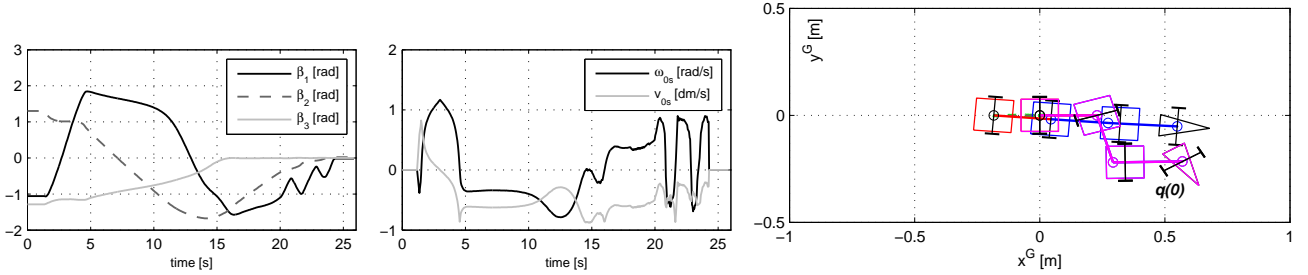


Figure 11: E2: experimental results of active lining-up maneuvers for GNT vehicle by using approximation (79) ($q(0)$ indicates the initial vehicle configuration highlighted in magenta)
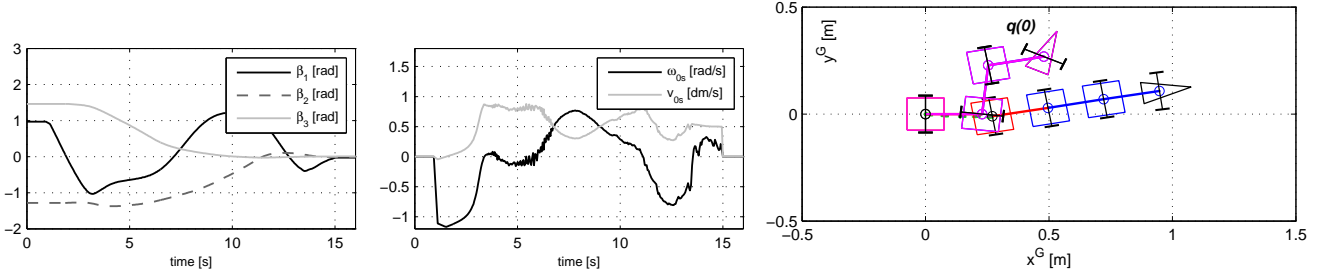


Figure 12: E3: experimental results of active lining-up maneuvers for SNT vehicle by using approximation (79) ($q(0)$ indicates the initial vehicle configuration highlighted in magenta)

In experiment E3, lining-up strategy has been tested also for the SNT vehicle with $L_{hi} = 0.0$, $i = 1, 2, 3$. In this case all the hitching offsets were equal to zero, thus approximation (79) was necessary for all three inverse matrices. Worth to note that either positive or negative approximating parameters $\varepsilon_i$ were admissible in this case (however, with a homogeneous sign). The following parameter values have been selected: $\varepsilon_1 = -0.008\,\text{m}$, and $\varepsilon_2 = \varepsilon_3 = -0.032\,\text{m}$. By selection of negative parameters one expects active lining-up maneuvers in the forward motion strategy (cf. (29)). Control performance for SNT vehicle can be assessed upon the plots in Fig. 12. Also in this case the cost of the approximation is reflected in a slight

drift of the last-trailer orientation ($\theta_3(T_a) \approx 9.9\,\text{deg}$), and in less smooth behavior of the tractor. Lining-up time-horizon and distance passed by the last segment have been assessed, respectively, as $T_a \approx 14.07\,\text{s}$, and $s_3(T_a) \approx 0.271\,\text{m}$ (the distance does not include a small movement along $y^G$ axis).

The last example, E4, provides the results of lining-up maneuvers for the GNT vehicle with utilization of mapping (81). In this case the following hitching offsets have been selected: $L_{h1} = L_{h2} = 0.048\,\text{m}$, and $L_{h3} = 0.0$. As a consequence, mapping (81) was implemented only for the third joint using coefficient $k_3 = 10$. Analyzing the plots in Fig. 13 one can find that the control performance
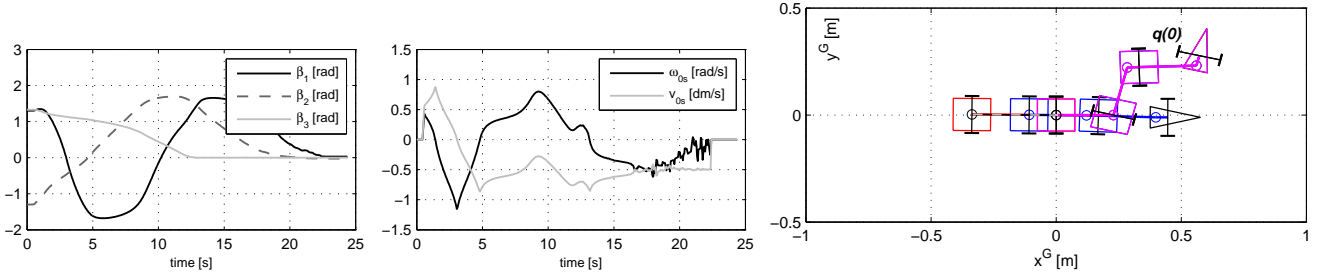
Figure 13: E4: experimental results of active lining-up maneuvers for GNT vehicle by using modification (81) for the last joint ($q(0)$ indicates the initial vehicle configuration highlighted in magenta)

obtained in this case is very similar to the results of experiment E1 (cf. Fig. 10) despite the on-axle hitching of the third trailer. The orientation angle of the last trailer has been almost preserved after the lining-up maneuvers, since $\theta_3(T_a) \approx -0.44 \deg$. The lining-up time-horizon and distance passed by the last segment have been assessed, respectively, as $T_a \approx 21.98\,\mathrm{s}$, and $s_3(T_a) \approx 0.337\,\mathrm{m}$ (the distance does not include a small movement along $y^G$ axis).

## 7 Conclusions

In the paper the active and passive lining-up control strategies for N-trailer robotic vehicles have been considered and compared. The active lining-up strategy has been proposed as a highly scalable feedback control law, in contrast to the conventional passive lining-up maneuvers which result from the open-loop control. It has been revealed that effectiveness of particular lining-up strategies principally depends on the kinematic parameter ratio $|L_{hi}|/L_i$, while the equivalence between the methods holds for $(|L_{hi}|/L_i) = 1$. Furthermore, it was shown that for the most common case where $(|L_{hi}|/L_i) \ll 1$ the active lining-up strategy is substantially more effective than the passive one. The main condition required for successful application of the active strategy, which restricts application of the method, is the sign-homogeneous hitching of all the trailers in a vehicle (the restriction does not pertain to the passive strategy). The active strategy has been proposed and analyzed for the nSNT kinematics. However, after simple modifications devised for the on-axle joints, applicability of the method has been extended also for GNT and SNT vehicles. Effectiveness of the active strategy has been validated by the results of laboratory experiments. Worth to note that application of the lining-up methods to vehicles equipped with a tractor of car-like kinematics is possible by using the control framework presented in [19].

## Appendix

### 7.1 Product of transformation matrices at equilibria

In order to show the forms of a product of transformation matrices (and their inverses) at the equilibria $\bar{\boldsymbol{\beta}} = [\bar{\beta}_1 \ \ldots \bar{\beta}_N]^\top$, $\bar{\beta}_i = 2k\pi$, $k = 0, \pm 1, \ldots$ one should note that (cf. (5) and (14)):

$$\boldsymbol{J}_i(\bar{\beta}_i) = \begin{bmatrix} -\frac{L_{hi}}{L_i}\mathrm{c}\bar{\beta}_i & 0 \\ 0 & \mathrm{c}\bar{\beta}_i \end{bmatrix}, \qquad (88)$$

$$\boldsymbol{J}_i^{-1}(\bar{\beta}_i) = \begin{bmatrix} -\frac{L_i}{L_{hi}}\mathrm{c}\bar{\beta}_i & 0 \\ 0 & \mathrm{c}\bar{\beta}_i \end{bmatrix}. \qquad (89)$$

Since the above matrices are diagonal it is evident that:

$$\prod_{j=i}^{1} \boldsymbol{J}_j(\bar{\beta}_j) \equiv \prod_{j=1}^{i} \boldsymbol{J}_j(\bar{\beta}_j) = \boldsymbol{J}_1(\bar{\beta}_1)\boldsymbol{J}_2(\bar{\beta}_2)\ldots\boldsymbol{J}_i(\bar{\beta}_i)$$
$$= \begin{bmatrix} (-1)^i \prod_{j=1}^{i} \frac{L_{hj}}{L_j}\mathrm{c}\bar{\beta}_j & 0 \\ 0 & \prod_{j=1}^{i} \mathrm{c}\bar{\beta}_j \end{bmatrix}, \quad (90)$$

and

$$\prod_{j=i}^{N} \boldsymbol{J}_j^{-1}(\bar{\beta}_j) = \boldsymbol{J}_i^{-1}(\bar{\beta}_i)\boldsymbol{J}_{i+1}^{-1}(\bar{\beta}_{i+1})\ldots\boldsymbol{J}_N^{-1}(\bar{\beta}_N)$$
$$= \begin{bmatrix} (-1)^{N-i+1} \prod_{j=i}^{N} \frac{L_j}{L_{hj}}\mathrm{c}\bar{\beta}_j & 0 \\ 0 & \prod_{j=i}^{N} \mathrm{c}\bar{\beta}_j \end{bmatrix}. \qquad (91)$$

### 7.2 Partial derivatives of matrices $\boldsymbol{J}_F(\cdot)$ and $\boldsymbol{J}_B(\cdot)$

Let us consider the form of partial derivatives $\frac{\partial \boldsymbol{J}_F(\beta_1,\ldots,\beta_{i-1})}{\partial \beta_k}$ and $\frac{\partial \boldsymbol{J}_B(\beta_{i+1},\ldots,\beta_N)}{\partial \beta_k}$ evaluated at equilibria $\bar{\boldsymbol{\beta}} = [\bar{\beta}_1 \ \ldots \bar{\beta}_N]^\top$, $\bar{\beta}_i = 2k\pi$, $k = 0, \pm 1, \ldots$, where the product matrices are determined, respectively, by $\boldsymbol{J}_F(\cdot) = \prod_{i-1}^{1} \boldsymbol{J}_j(\beta_j)$ and $\boldsymbol{J}_B(\cdot) = \prod_{i+1}^{N} \boldsymbol{J}_j^{-1}(\beta_j)$.

Since $\boldsymbol{J}_F(\beta_1,\ldots,\beta_{i-1}) \triangleq \prod_{j=i-1}^{1} \boldsymbol{J}_j(\beta_j)$ and since $\prod_{j=i}^{1} \boldsymbol{J}_j(\bar{\beta}_j) \equiv \prod_{j=1}^{i} \boldsymbol{J}_j(\bar{\beta}_j)$ (because $\boldsymbol{J}_j(\bar{\beta}_j)$ are diagonal matrices) then (using notation $\bar{\boldsymbol{J}}_j \equiv \boldsymbol{J}_j(\bar{\beta}_j)$ for compact-

ness):

$$\left.\frac{\partial \boldsymbol{J}_F(\cdot)}{\partial \beta_k}\right|_{\boldsymbol{\beta}=\bar{\boldsymbol{\beta}}} = \bar{\boldsymbol{J}}_{i-1} \ldots \bar{\boldsymbol{J}}_{k+1} \frac{d\boldsymbol{J}_k}{d\beta_k}(\bar{\beta}_k) \bar{\boldsymbol{J}}_{k-1} \ldots \bar{\boldsymbol{J}}_1$$

$$\equiv \bar{\boldsymbol{J}}_{k+1} \ldots \bar{\boldsymbol{J}}_{i-1} \frac{d\boldsymbol{J}_k}{d\beta_k}(\bar{\beta}_k) \bar{\boldsymbol{J}}_1 \ldots \bar{\boldsymbol{J}}_{k-1}$$

$$= \prod_{j=k+1}^{i-1} \bar{\boldsymbol{J}}_j \cdot \frac{d\boldsymbol{J}_k}{d\beta_k}(\bar{\beta}_k) \cdot \prod_{j=1}^{k-1} \bar{\boldsymbol{J}}_j$$

$$= \prod_{j=k+1}^{i-1} \bar{\boldsymbol{J}}_j \cdot \begin{bmatrix} 0 & \frac{1}{L_k}\mathrm{c}\bar{\beta}_k \\ L_{hk}\mathrm{c}\bar{\beta}_k & 0 \end{bmatrix} \cdot \prod_{j=1}^{k-1} \bar{\boldsymbol{J}}_j$$

$$= \begin{bmatrix} 0 & \left.\frac{\partial p_{12}(\cdot)}{\partial \beta_k}\right|_{\boldsymbol{\beta}=\bar{\boldsymbol{\beta}}} \\ \left.\frac{\partial p_{21}(\cdot)}{\partial \beta_k}\right|_{\boldsymbol{\beta}=\bar{\boldsymbol{\beta}}} & 0 \end{bmatrix} \quad (92)$$

with

$$\left.\frac{\partial p_{21}(\cdot)}{\partial \beta_k}\right|_{\boldsymbol{\beta}=\bar{\boldsymbol{\beta}}} = (-1)^{k-1} L_{hk} \prod_{j=1}^{i-1} \mathrm{c}\bar{\beta}_j \prod_{j=1}^{k-1} \frac{L_{hj}}{L_j}, \quad (93)$$

$$\left.\frac{\partial p_{12}(\cdot)}{\partial \beta_k}\right|_{\boldsymbol{\beta}=\bar{\boldsymbol{\beta}}} = (-1)^{i-k-1} \frac{1}{L_k} \prod_{j=1}^{i-1} \mathrm{c}\bar{\beta}_j \prod_{j=k+1}^{i-1} \frac{L_{hj}}{L_j}, \quad (94)$$

where the following formulas have been used:

$$\prod_{j=k+1}^{i-1} \boldsymbol{J}_j(\bar{\beta}_j) \overset{(90)}{=} \begin{bmatrix} (-1)^{i-k-1} \prod_{j=k+1}^{i-1} \frac{L_{hj}}{L_j}\mathrm{c}\bar{\beta}_j & 0 \\ 0 & \prod_{j=k+1}^{i-1} \mathrm{c}\bar{\beta}_j \end{bmatrix},$$

$$\prod_{j=1}^{k-1} \boldsymbol{J}_j(\bar{\beta}_j) \overset{(90)}{=} \begin{bmatrix} (-1)^{k-1} \prod_{j=1}^{k-1} \frac{L_{hj}}{L_j}\mathrm{c}\bar{\beta}_j & 0 \\ 0 & \prod_{j=1}^{k-1} \mathrm{c}\bar{\beta}_j \end{bmatrix}.$$

By analogy, $\boldsymbol{J}_B(\beta_{i+1}, \ldots, \beta_N) \triangleq \prod_{j=i+1}^N \boldsymbol{J}_j^{-1}(\beta_j)$ thus (using notation $\bar{\boldsymbol{J}}_j^{-1} \equiv \boldsymbol{J}_j^{-1}(\bar{\beta}_j)$ for compactness):

$$\left.\frac{\partial \boldsymbol{J}_B(\cdot)}{\partial \beta_k}\right|_{\boldsymbol{\beta}=\bar{\boldsymbol{\beta}}} = \bar{\boldsymbol{J}}_{i+1}^{-1} \ldots \bar{\boldsymbol{J}}_{k-1}^{-1} \frac{d\boldsymbol{J}_k^{-1}}{d\beta_k}(\bar{\beta}_k) \bar{\boldsymbol{J}}_{k+1}^{-1} \ldots \bar{\boldsymbol{J}}_N^{-1}$$

$$= \prod_{j=i+1}^{k-1} \bar{\boldsymbol{J}}_j^{-1} \cdot \frac{d\boldsymbol{J}_k^{-1}}{d\beta_k}(\bar{\beta}_k) \cdot \prod_{j=k+1}^{N} \bar{\boldsymbol{J}}_j^{-1}$$

$$= \prod_{j=i+1}^{k-1} \bar{\boldsymbol{J}}_j^{-1} \cdot \begin{bmatrix} 0 & \frac{1}{L_{hk}}\mathrm{c}\bar{\beta}_k \\ L_k\mathrm{c}\bar{\beta}_k & 0 \end{bmatrix} \cdot \prod_{j=k+1}^{N} \bar{\boldsymbol{J}}_j^{-1}$$

$$= \begin{bmatrix} 0 & \left.\frac{\partial r_{12}(\cdot)}{\partial \beta_k}\right|_{\boldsymbol{\beta}=\bar{\boldsymbol{\beta}}} \\ \left.\frac{\partial r_{21}(\cdot)}{\partial \beta_k}\right|_{\boldsymbol{\beta}=\bar{\boldsymbol{\beta}}} & 0 \end{bmatrix} \quad (95)$$

with

$$\left.\frac{\partial r_{21}(\cdot)}{\partial \beta_k}\right|_{\boldsymbol{\beta}=\bar{\boldsymbol{\beta}}} = (-1)^{N-k} L_k \prod_{j=i+1}^{N} \mathrm{c}\bar{\beta}_j \prod_{j=k+1}^{N} \frac{L_j}{L_{hj}}, \quad (96)$$

$$\left.\frac{\partial r_{12}(\cdot)}{\partial \beta_k}\right|_{\boldsymbol{\beta}=\bar{\boldsymbol{\beta}}} = (-1)^{k-i-1} \frac{1}{L_{hk}} \prod_{j=i+1}^{N} \mathrm{c}\bar{\beta}_j \prod_{j=i+1}^{k-1} \frac{L_j}{L_{hj}}, \quad (97)$$

where the following formulas have been used:

$$\prod_{j=i+1}^{k-1} \boldsymbol{J}_j^{-1}(\bar{\beta}_j) \overset{(91)}{=} \begin{bmatrix} (-1)^{k-i-1} \prod_{j=i+1}^{k-1} \frac{L_j}{L_{hj}}\mathrm{c}\bar{\beta}_j & 0 \\ 0 & \prod_{j=i+1}^{k-1} \mathrm{c}\bar{\beta}_j \end{bmatrix},$$

$$\prod_{j=k+1}^{N} \boldsymbol{J}_j^{-1}(\bar{\beta}_j) \overset{(91)}{=} \begin{bmatrix} (-1)^{N-k} \prod_{j=k+1}^{N} \frac{L_j}{L_{hj}}\mathrm{c}\bar{\beta}_j & 0 \\ 0 & \prod_{j=k+1}^{N} \mathrm{c}\bar{\beta}_j \end{bmatrix}.$$

# References

[1] C. Altafini. Some properties of the general n-trailer. *Int. Journal of Control*, 74(4):409–424, 2001.

[2] C. Altafini. Following a path of varying curvature as an output regulation problem. *IEEE Trans. on Automatic Control*, 47(9):1551–1556, 2002.

[3] A. Astolfi, P. Bolzern, and A. Locatelli. Path-tracking of a tractor-trailer vehicle along rectilinear and circular paths: a Lyapunov-based approach. *IEEE Trans. on Robotics and Automation*, 20(1):154–160, 2004.

[4] P. Bolzern, R. M. DeSantis, A. Locatelli, and D. Masciocchi. Path-tracking for articulated vehicles with off-axle hitching. *IEEE Trans. on Control Systems Technology*, 6(4):515–523, 1998.

[5] F. Bullo and R. M. Murray. Experimental comparison of trajectory trackers for a car with trailers. In *13th IFAC World Congress*, pages 407–412, San Francisco, USA, 1996.

[6] W. Chung, M. Park, K. Yoo, J. I. Roh, and J. Choi. Backward-motion control of a mobile robot with $n$ passive off-hooked trailers. *J. Mechanical Science and Technology*, 25(11):2895–2905, 2011.

[7] F. Cuesta, F. Gomez-Bravo, and A. Ollero. Parking maneuvers of industrial-like electrical vehicles with and without trailer. *IEEE Trans. on Industrial Electronics*, 51(2):257–269, 2004.

[8] A. Isidori. *Nonlinear Control Systems II.* Springer, London, 1999.

[9] F. Jean. The car with N trailers: characterisation of the singular configurations. *Control, Opt. Calc. Variations*, 1:241–266, 1996.

[10] J. P. Laumond. Controllability of a multibody mobile robot. *IEEE Trans. on Robotics and Automation*, 9(6):755–763, 1993.

[11] D. A. Lizarraga, P. Morin, and C. Samson. Chained form approximation of a driftless system. Application to the exponential stabilization of the general n-trailer system. *Int. Journal of Control*, 74(16):1612–1629, 2001.

[12] J. L. Martinez, J. Morales, A. Mandow, and A. Garcia-Cerezo. Steering limitations for a vehicle pulling passive trailers. *IEEE Trans. on Control Systems Technology*, 16(4):809–818, 2008.

[13] R. T. M'Closkey and R. M. Murray. Experiments in exponential stabilization of a mobile robot towing a trailer. In *Proc. of the American Control Conf.*, pages 988–993, Baltimore, USA, 1994.

[14] M. Michalek. Geometrically motivated set-point control strategy for the standard N-trailer vehicle. In *2011 IEEE Intelligent Vehicles Symposium*, pages 138–143, Baden-Baden, Germany, 2011.

[15] M. Michalek. Active and passive straightening control strategies for non-standard N-trailer vehicles. In *2012 IEEE Int. Conf. on Control Applications*, pages 1572–1577, Dubrovnik, Croatia, 2012.

[16] M. Michalek. Application of the VFO method to set-point control for the N-trailer vehicle with off-axle hitching. *Int. Journal of Control*, 85(5):502–521, 2012.

[17] M. Michalek. Non-minimum-phase property of N-trailer kinematics resulting from off-axle interconnections. *Int. Journal of Control*, 86(4):740–758, 2013.

[18] M. Michalek and K. Kozlowski. Vector-Field-Orientation feedback control method for a differentially driven vehicle. *IEEE Trans. on Control Systems Technology*, 18(1):45–65, 2010.

[19] M. Michalek and K. Kozlowski. Feedback control framework for car-like robots using the unicycle controllers. *Robotica*, 30:517–535, 2012.

[20] J. Morales, J. L. Martinez, A. Mandow, and A. J. Garcia-Cerezo. Steering the last trailer as a virtual tractor for reversing vehicles with passive on- and off-axle hitches. *IEEE Trans. Industrial Electronics*, 2013.

[21] C. Pradalier and K. Usher. Robust trajectory tracking for a reversing tractor trailer. *Journal of Field Robotics*, 25(6-7):378–399, 2008.

[22] J. I. Roh and W. Chung. Reversing control of a car with a trailer using the driver assistance system. *Int. J. Advanced Robotic Systems*, 8(2):114–121, 2011.

[23] S. Skogestad and I. Postlethwaite. *Multivariable feedback control. Analysis and design. Second Ed.* John Wiley and Sons, Ltd, 2007.

[24] O. J. Sordalen and K. Y. Wichlund. Exponential stabilization of a car with $n$ trailers. In *Proceedings of the 32th Conf. on Decision and Control*, pages 978–983, San Antonio, USA, 1993.

[25] R. Stahn, G. Heiserich, and A. Stopp. Laser scanner-based navigation for commercial vehicles. In *Proc. of the 2007 IEEE Intell. Vehicles Symposium*, pages 969–974, Istanbul, Turkey, 2007.

[26] I. A. Tall. Feedback linearizable feedforward systems: A special class. *IEEE Trans. Automatic Control*, 55:1736–1742, 2010.

[27] I. A. Tall and W. Respondek. Transforming a single input nonlinear system to a feedforward form via feedback. In A. Isidori, F. Lamnabhi-Lagarrigue, and W. Respondek, editors, *Nonlinear Control in the Year 2000*, pages 527–542. Springer, 2000.

[28] K. Tanaka, S. Hori, and H. O. Wang. Multiobjective control of a vehicle with triple trailers. *IEEE/ASME Trans. on Mechatronics*, 7(3):357–368, 2002.